30 DECEMBER, 1991

THE FOX ISLAND RIVER CHROMITE PLACER SURVEY - NOVEMBER 1991

by

Carl L. Amos
Geological Survey of Canada
Bedford Institute of Oceanography
Dartmouth, N.S., B2Y 4A2

a field report prepared for:

C-CORE
Memorial University of Newfoundland
St. John's, Newfoundland,
B3H 4J1

unpublished report

THE FOX ISLAND RIVER CHROMITE PLACER SURVEY - NOVEMBER 1991

by

Carl L. Amos
Geological Survey of Canada
Bedford Institute of Oceanography
Dartmouth, N.S., B2Y 4A2

SEA CAROUSEL

System Configuration - Sea Carousel

Sea Carousel, named after the carousels of Postma (1967) and Hydraulic Research Limited (Burt, 1984), is a benthic annular flume designed for field use in intertidal and subtidal settings. The carousel is 1.0 m in radius with an annulus 0.15 m wide and 0.30 m high (Figure 1). It weighs approximately 150 kg in air and 40 kg in water and is made entirely of aluminium. Flow in the annulus is induced by rotating a movable lid that is driven by a 0.35 hp DC motor powered from the surface. Eight small paddles, spaced equidistantly beneath the lid, induce a flow of water in the annulus. The width of the annulus (D) was made 0.15 m to give a relative roughness (e/D) $\approx$ 0.004 (where the wall roughness, e $\approx$ 0.0006 m; after Shames, 1962). The water depth in the annulus was minimized to 0.25 m to ensure conditions for Nikuradse's "rough-pipe zone of flow" wherein changes in wall friction factor with changes in Reynolds number are at a minimum (Shames, 1962).

A schematic diagram of the Sea Carousel configuration is shown in Figure 2. It is equipped with three optical backscatter sensors (OBS's; Downing, 1983). Two of these are located non-intrusively on the inner wall of the annulus at heights of 0.03 and 0.18 m above the skirt (the skirt is a horizontal flange situated around the outer wall of the annulus 0.04 m above the base; it was designed to standardize penetration of the flume into the seabed; see Figure 1). The third OBS detects ambient particle concentration outside the annulus, or it may be used to detect internal sediment concentration at a height between the other two. The OBS sensors give linear responses to particle concentration (of a constant size) for both mud and sand over a concentration range of 0.1 to 50 g/L (Downing and Beach, 1989). They are unaffected by flows below 1.5 m/s and are stable through time. A sampling port is situated in the outer wall of the annulus at a height of 0.2 m above the skirt through which water samples can be drawn to calibrate the three sensors under well mixed conditions.

A Marsh/McBirney current meter (model 511) is located on the centreline of the annulus at a height of 0.16 m above the skirt. It

was used to detect the instantaneous azimuthal and vertical components of flow within the annulus (U_y and U_w respectively). Mean tangential lid rotational speed ($\bar{U}_r$) is detected through a shaft encoder that runs on the lid. Controller boards for each sensor and the necessary power (12 VDC) are derived from an underwater pod located above the annulus. Output voltages from all sensors are digitized and transformed to scientific units on a Campbell Scientific CR10 data logger and stored on a Campbell Scientific SM192 storage module (storage capacity of 96,000 data values), also located in the underwater pod. The data logger is interrogated and programmed from the surface using a microcomputer linked to the data logger through an RS232 interface. Maximum sampling rate of all channels is approximately 2 Hz, whereas U_y and U_w may be logged at rates up to 10.66 Hz. All channels may be monitored and displayed on the surface computer allowing the operator to control the experiment interactively. Bed shear stress is varied in time by varying the power supplied to the underwater motor up to 350 watts via a surface power supply. The data stored from each deployment may be downloaded remotely through the RS232 cable at the end of each experiment and the storage module re-initialized.

A window is located in the inner flume wall for purposes of observing and recording the mechanics of bed failure. A perspex wedge at the base of the window sections the sediment upon deployment. Thus the upper 20 mm of sediment and the lower 10 cm of the water column can be viewed in section. Visual observations are made using an Osprey underwater SIT black and white camera; records are displayed using a surface monitor. Light is provided by two 100 watt underwater lights powered from the surface. The housing has a lens that corrects for underwater geometric distortions and so is suitable for accurate image scaling. The camera lens is located approximately 20 mm from the window. Horizontal and vertical scale lines are present on the window and situated within the field of view. The camera images 30 frames/s. A co-axial cable connects the camera to a surface monitor for real-time detection. Video records are stored on a standard VHS video cassette recorder also at the surface. Sequential video images are digitized for particle trajectories at varying heights above the bed. From these, velocity profiles are constructed.

The root-mean-square value of the time and width averaged friction velocity ($\bar{U}_*rms$) is correlated with $\bar{U}_y$. The relationship of $\bar{U}_*rms$ and $\bar{U}_y$ is good, and takes the form:

$$\bar{U}_*rms = 0.0167 + 0.097\bar{U}_y \quad (m/s;\ r^2 = 0.96) \qquad (1)$$

Thus $\bar{U}_*rms$ is used as the standard hydrodynamic measure in this study. By manipulation of the quadratic stress law a drag coefficient (C_d) relating $\bar{U}_y$ and $\bar{U}_*$ is derived:

$$\bar{U}_*rms = \sqrt{\tau/\rho} \qquad (2)$$

and $\tau = C_d \rho \bar{U}_y^2$ (3)

thus $C_d = \tau / \rho \bar{U}_y^2 = \bar{U}_* rms^2 / \bar{U}_y^2$ (4)

This results in a value of $C_d = 4.0 \times 10^{-2}$ and a corresponding C_{d100} of 1.3×10^{-3}. The latter coefficient falls within the range of values detected over flat bed in the field observations of Sternberg (1972).

Water samples were pumped at intervals from a port located in the side of Sea Carousel at a height of approximately 20 cm above the bed. These water samples were then filtered for total suspended particulate matter in order to calibrate the OBS sensors and to provide sample material of suspended material. A detailed description of the system is given in Amos *et al.* (in press) and results measured in the Bay of Fundy are presented in Amos *et al.* (in review).

System Configuration - SOBS

SOBS (Submersible Observatory of Benthic Stability) is a benthic tripod equipped with six Optical Backscatter Sensors (OBS's) that detect sediments in suspension (Figure 3). The sensors are arranged in a logarithmic progression from a height of 10 cm above the bed to 200 cm (item 6). Sensor 1 (10 cm) looks downards and is designed to detect ripple mobilization and bedload transport. From it we can obtain the onset of bed motion. Sensors 2 - 6 are arranged to monitor in the horizontal plane at heights above the bed of 11 cm, 38 cm, 82 cm, 136 cm, and 200 cm respectively. Data from each sensor are logged on an underwater Tattletale data logger at a rate of 1 Hz (item 5). At this rate, the instrument can collect data for 19.3 days before saturating the memory. An underwater video camera (Sony V101, item 1) and Amphibico flood lights (item 2) are also located on the tripod. The camera can burst sample the bed at programmable intervals and durations. This is controlled by the underwater Tattletale. A scale is located in the field of view for reference (item 7). Finally, an InterOcean S4 current meter (item 3) is mounted on a independent frame to provide data on wave height and mean currents. The current meter is programmed independently of the SOBS system. Power is provided by a submersible 12 v battery pack (item 4). The whole system is weighted at the feet for stability (items 8 and 9).

The SOBS is normally deployed with a 50 m ground line, and is marked with a header float (Figure 4). The current meter frame is usually located at the end of the ground line, and is also marked with a header float.

RESULTS

Sea Carousel

Eight successful deployments of Sea Carousel were carried out in the nearshore region off Fox Island River. GPS was not available at the

time and so uncalibrated Loran-C was used for positioning. FIR1 was situated adjacent to the INRS S4 current meter mooring immediately off the mouth of Fox Island River; FIR2, FIR7 and FIR8 were situated along a shore-normal transect that passed throught the SOBS site, approximately 2 km south of Fox Island River. FIR3, FIR4, FIR5 and FIR6 were located at positions along the shoreface south of Fox Island River. The following table reviews the stations occupied in this study:

TABLE 1. A summary of stations occupied by Sea Carousel in this study.

STATION	DATE	DURATION(h)	DEPTH(m)	LAT	LON
FIR1	23 NOV. 1991	1:28	10	off river mouth (S4 site)	
FIR2	23 NOV. 1991	1:10	7	SOBS site 2 km south of river mouth	
FIR3	23 NOV. 1991	1:34	8	48 38.83	58 40.95
FIR4	23 NOV. 1991	1:17	8	48 41.04	58 42.10
FIR5	24 NOV. 1991	1:12	8	48 36.46	58 41.32
FIR6	24 NOV. 1991	1:21	6	48 37.59	58 40.53
FIR7	24 NOV. 1991	1:21	4	48 39.95	58 41.11
FIR8	24 NOV. 1991	1:04	20	48 39.85	58 41.61

Approximately eight water samples were pumped during the course of each deployment. The times of pumping and the total suspended sediment concentration (dry weight) are given in Table 2.

TABLE 2. Suspended sediments pumped from Sea Carousel during the eight deployments of this study.

TIME (AST)	SSC (mg/L)	TIME (AST)	SSC (mg/L)	TIME (AST)	SSC (mg/L)
FIR1		FIR2		FIR3	
1300	6.7	1509	34.6	1701	54.7
1318	26.5	1512	183	1718	33.7
1334	18.7	1521	330	1731	249
1343	491	1536	403	1742	140
1348	35.2	1542	512	1754	246
1358		1552	1007	1805	224
		1602	723	1817	209

TIME (AST)	SSC (mg/L)	TIME (AST)	SSC (mg/L)	TIME (AST)	SSC (mg/L)
FIR4		FIR5		FIR6	
1931	94.4	1054	51.4	1239	137
1936	41.0	1105	165	1244	101
1942	29.1	1112	227	1249	123
1951	30.3	1118	364	1254	243
1958	167	1127	395	1300	375
2012	250	1133	284	1308	670
2022	224	1137	467	1314	420
2028	273	1142	654	1320	367
		1148	962	1326	561
				1332	526
FIR7		FIR8		1338	1029
1446	118	1712	601	1345	778
1456	87	1716	402	1350	1065
1502	196	1721	656		
1508	190	1728	1091		
1514	417	1734	1220		
1520	225	1742	998		
1527	374	1752	744		
1534	357	1757	503		
1540	325				
1546	188				
1552	369				
1600	420				

Suspended masses measured on the filtered samples were regressed against the OBS voltage readings to derive total suspended mass in the flume. Plots of the regression analysis for the sand calibration (FIR1 - FIR7) and silt calibration (FIR8) are shown respectively in Figures 5A and B.

The calibration functions so derived were as follows for stations

FIR1 to FIR7:

$$SSC(1) = -18 + 3.25(OBS1) - 0.013(OBS1)^2 + 0.00004(OBS1)^3 \; ; \; r = 0.91 \quad (5)$$

$$SSC(3) = -18 + 3.25(OBS3) - 0.013(OBS3)^2 + 0.00004(OBS3)^3 \; ; \quad (5A)$$

The same calibration was used for both sensors despite differences in sensor responses. Sensor 3 (lower) always indicated a higher voltage than the sensor 1 (upper). Previous calibrations indicate this is not due to differences in electronic responses, but rather to a gradient in sand concentration with height above the bed. The higher scatter in results from sensor 3 suggest a greater sensitivity to bursts and sweeps of random turbulent events.

The calibration functions of OBS voltage to suspended silt (from FIR8) takes the form:

$$SSC(1) = -66.4 + 3.92(OBS1); \; r = 0.98 \quad (6)$$

$$SSC(3) = -66.4 + 3.92(OBS3); \quad (6A)$$

SSC(1) and SSC(3) refer to the suspended sediment concentration inside the annulus recorded by the upper and lower sensors respectively. OBS sensor 2 was situated outside the annulus and gave a measure of the ambient bottom water suspended concentration. Only one ambient water sample was collected during the course of each experiment and so a calibration curve was not derived.

The results of the Sea Carousel deployments provide information on

1. the presence or absence of bedforms and benthic fauna at the time of deployment (as seen on the video camera),

2. surface shear strength for traction and suspension (or resistance to erosion) of the seabed,

3. the resistance of the seabed to scour to depths of approximately 5 cm below the seabed, and

4. the degree of bed consolidation (intuitively through the internal friction angle) i.e. consolidated, unconsolidated, or gel states.

The stresses imposed on the bed are artificial, however the bed responses are real and representative. We emphasise that to put these results into a long-term context specific to the west coast of Newfoundland we need to know the return interval of each imposed bed stress. This can only be derived from long-term measures of the wave and current conditions.

Three illustrations of for each deployment site are given in the appendix. These are:

1. (A) the time series of azimuthal and vertical current speed induced in the flume (m/s); (B) the raw and cumulative suspended sediment concentration from the 3 OBS's (mg/L); and (C) the erosion rate (differential in sediment concentration in $kg/m^2/s$).

2. Results of the deployment shown on a Mohr-Coulomb plot (applied bed stress (Pa) versus effective stress (Pa)). The effective stress is proportional to depth in the sediment. The solid lines in the figures trace the failure envelope of the sediment with depth (i.e. increase in sediment shear strength). The slope of the line is equivalent to the friction angle of the sediment and is a direct indicator of sediment density, and the intercept is the critical shear stress for sediment suspension. The scatter in results about the failure envelop is a measure of the variability in grain-to-grain pivotal angle as the erosion process proceeds. It is diagnostic, therefore, of the degree of sorting in size, shape and density of bed material.

3. The relationship of erosion rate (into suspension) to applied bed shear stress. This relationship is important to the prediction of bed stability. Note that it does not include bedload transport which has yet to be determined through the video records.

Bedload transport and ripple migration were observed to occur in the video data. In order to derive the threshold for incipient motion (or traction) one must refer to these tapes. This is planned for 1992.

Results - Sea Carousel

The main parameters derived from this study are: surface shear strength, also known as the critical shear stress for sediment suspension; friction angle; consolidation profile with depth; and erosion rate as a function of applied bed stress. Table 3 summarizes the results derived from the 10 deployments of Sea Carousel:

TABLE 3. A summary of results of sediment stability from the Sea Carousel deployments undertaken in this study.

STATION	TAUCRIT (Pa)	EROSION RATE(E) ($kg/m^2/s$)	APPARENT FRICTION ANGLE (degrees)
FIR1	2.9	10^{-4} TO 10^{-3}	74°
FIR2	1.1	10^{-3}	16°
FIR3	1.0	10^{-4} TO 10^{-3}	60°
FIR4	2.5	10^{-4} TO 10^{-3}	59°
FIR5	1.3	10^{-4} TO 5 x 10^{-3}	45°
FIR6	1.3	10^{-4} TO 10^{-3}	53°
FIR7	1.8	10^{-4} TO 10^{-3}	26°
FIR8	1.5	10^{-3}	29°

Good results were obtained from the 8 Sea Carousel deployment sites. Our tentative results show that the sediments at all sites were mobilized during the deployment of the Sea Carousel. The most stable sediments were found at FIR1: the region of coarse sand. This is verified by the high friction angle, the highest critical shear stress for erosion (TAUCRIT), and low erosion rates. FIR1 showed a moderate exponential relationship between erosion rate (E) and applied bed shear stress (τ) in the form:

$$E = (2.40 \times 10^{-5}) \times 1.45^{\tau} \ kg/m^2/s \quad (7)$$

FIR2, the SOBS site, exhibited the least degree of stability. This was apparent in the low critical shear stress for incipient motion (1.1 Pa), the lowest friction angle detected in the survey (16°), and the highest mean erosion rates (by approximately an order of magnitude). Erosion rates and critical stresses were similar to those detected at the silty site in 20 m of water along the SOBS transect. FIR2 showed no clear relationship between erosion rate and applied bed stress.

FIR4 was the second most stable sediment studied. It too had a high internal friction angle and relative low erosion rate. This friction angle varied significantly with depth indicating a complex sediment microfabric. The erosion rate showed a modest positive relationship to applied bed stress of the exponential form:

$$E = (3.63 \times 10^{-5}) \times 1.53^{\tau} \ kg/m^2/s \quad (8)$$

FIR5 was of intermediate stability, but showed a good relationship of erosion rate to bed shear stress in the exponential form:

$$E = (2.69 \times 10^{-5}) \times 1.91^{\tau} \ kg/m^2/s \quad (9)$$

FIR7 showed a constant friction angle with depth. The scatter in the Mohr-Coulomb plot probably indicates changes in grain-to-grain pivotal angle related to size shape and density. An exponential relationship of erosion rate to applied bed stress was also measured here:

$$E = (5.0 \times 10^{-5}) \times 1.52^{\tau} \text{ kg/m}^2\text{/s} \quad (10)$$

Notice that in most cases the base of the exponent remains very close to 1.5.

All remaining stations showed bed stabilities intermediate between the two extremes, both in terms of the erosion threshold and the internal friction angle. The rate of erosion for each deployment was consistent over the range of applied stresses, suggesting that a constant relationship may be adopted for modelling purposes once threshold conditions are exceeded.

Liquefaction (undrained failure) of the bed (zero friction angle) occurred only at higher stress at stations FIR2, FIR4, and FIR6. In all other cases, and at low stresses grain-to-grain contact of bed particles was maintained (drained failure). Increases in friction angle occurred in some cases with depth (stations FIR2 and FIR8). This reflects changes in bed composition or density reflecting the microfabric of the bed sediment at these sites.

Results - SOBS

Started: 0940 NST, 23 November, 1991
Deployed: 1030 NST, 23 November, 1991

Recovered: 0920 NST, 27 November, 1991
Stopped: 1037 NST, 27 November, 1991

The video camera was set up to record for 10 seconds every 5 minutes. The OBS sensors were logged continuously at 1Hz. The S4 current meter logged two horizontal components of flow and water depth every 2 seconds at a height of 50 cm above the seabed.

The current meter was pulled over during the deployment of the system. Consequently, no meaningful data were recovered at this site presumably because some if its electrodes were in the sediment. The SOBS data was successfully downloaded from the Tattletale which indicated that the system worked throughout. The camera failed almost immediately. This we attribute to condensation in the canister due to the large changes in temperature it experienced.

REFERENCES

Amos, C.L., Daborn, G.R., H.A. Christian, A. Atkinson, and A. Robertson. in review. Insitu erosion measurements on fine-grained sediments from the Bay of Fundy. Marine Geology.

Amos, C.L., Grant, J, Daborn, G.R., and Black, K. in press. Sea Carousel - a benthic annular flume. Estuarine Coastal and Shelf Sciences.

Burt, T.N. 1984. The Carousel: commissioning of a circular flume for sediment transport research. Hydraulic Research Limited Report SR 33.

Downing, J.P. 1983. An optical instrument for monitoring suspended particulates in ocean and laboratory. in Proceedings of Oceans'83: 199-202.

Downing, J.P. and Beach, R.A. 1989. Laboratory apparatus for calibrating optical suspended solids sensors. Marine Geology 86: 243 - 249.

Postma, H. 1967. Sediment transport and sedimentation in the estuarine environment. in Lauff, G.M. (ed), Estuaries. Publ. American Association for the Advancement of Science, No. 83: 158-179.

Shames, I. 1962. Mechanics of Fluids. Publ. McGraw-Hill Book Company,New York: 555p.

Sternberg, R.W. 1972. Predicting initial motion and bedload transport of sediment particles in the shallow marine environment. in D.J.P. Swift, D.B. Duane and O.H. Pilkey (eds) Shelf Sediment Transport, Processes and Pattern, Publ. Dowden, Hutchinson and Ross: 61-83.

APPENDIX - FIGURES

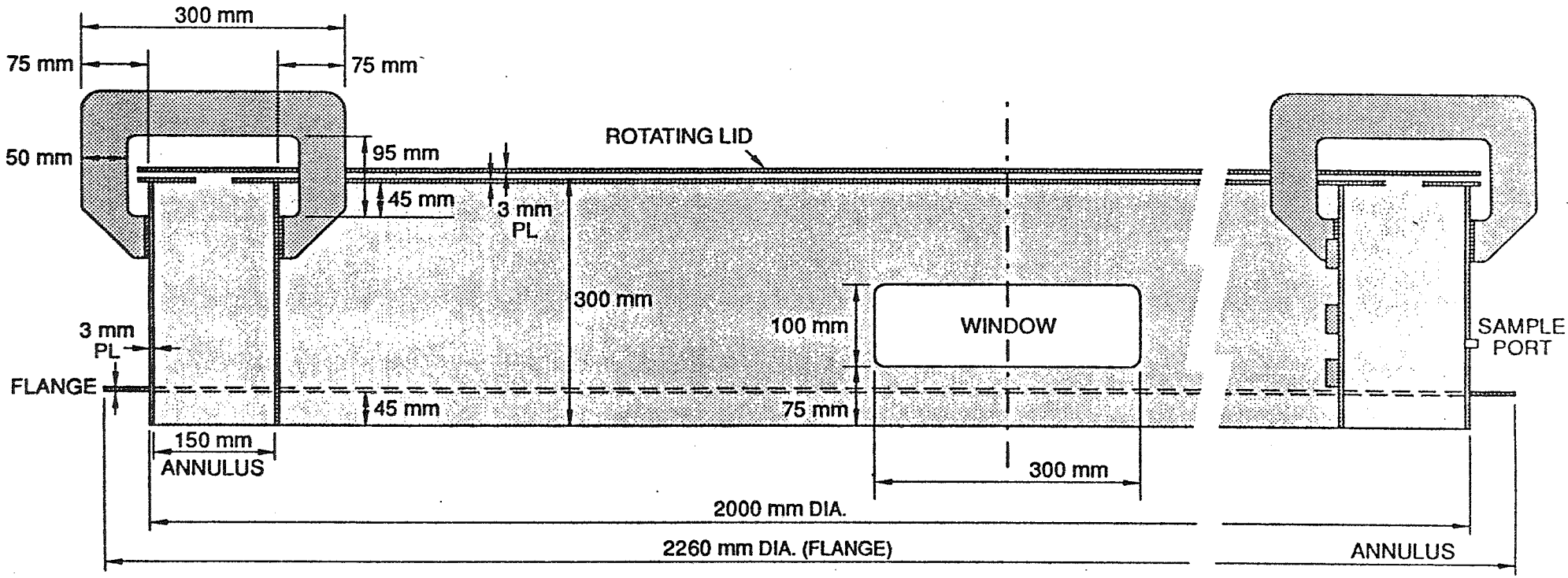
300 mm
75 mm
75 mm
50 mm
95 mm
45 mm
3 mm
PL
ROTATING LID
300 mm
100 mm
WINDOW
3 mm
PL
FLANGE
45 mm
75 mm
150 mm
ANNULUS
300 mm
2000 mm DIA.
2260 mm DIA. (FLANGE)
SAMPLE
PORT
ANNULUS

FIGURE 1

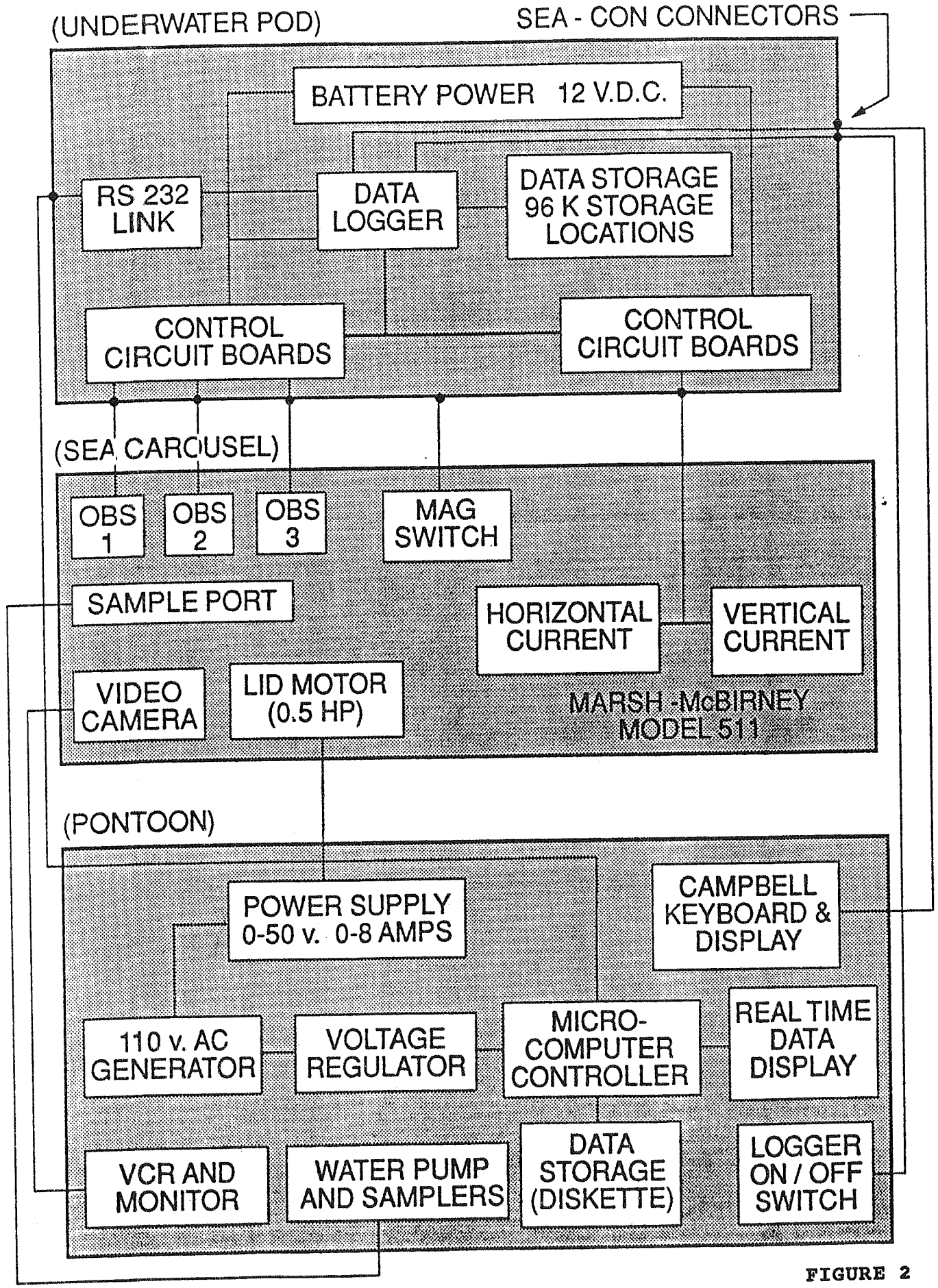
(UNDERWATER POD)
SEA - CON CONNECTORS
BATTERY POWER 12 V.D.C.
RS 232 LINK
DATA LOGGER
DATA STORAGE 96 K STORAGE LOCATIONS
CONTROL CIRCUIT BOARDS
CONTROL CIRCUIT BOARDS
(SEA CARCUSEL)
OBS 1
OBS 2
OBS 3
MAG SWITCH
SAMPLE PORT
HORIZONTAL CURRENT
VERTICAL CURRENT
VIDEO CAMERA
LID MOTOR (0.5 HP)
MARSH -McBIRNEY MODEL 511
(PONTOON)
POWER SUPPLY 0-50 v. 0-8 AMPS
CAMPBELL KEYBOARD & DISPLAY
110 v. AC GENERATOR
VOLTAGE REGULATOR
MICRO-COMPUTER CONTROLLER
REAL TIME DATA DISPLAY
VCR AND MONITOR
WATER PUMP AND SAMPLERS
DATA STORAGE (DISKETTE)
LOGGER ON / OFF SWITCH

FIGURE 2

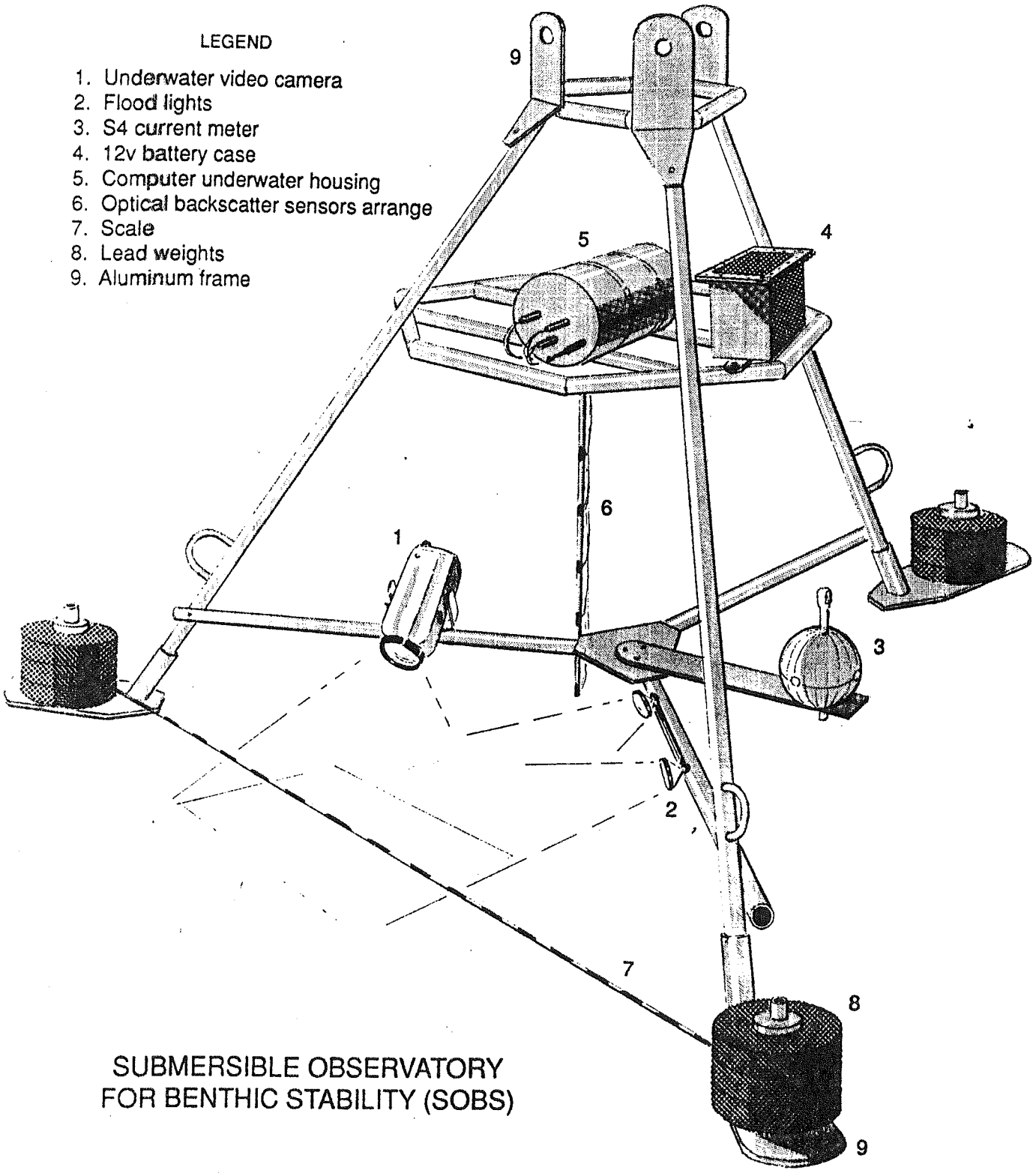
LEGEND
1. Underwater video camera
2. Flood lights
3. S4 current meter
4. 12v battery case
5. Computer underwater housing
6. Optical backscatter sensors arrange
7. Scale
8. Lead weights
9. Aluminum frame
SUBMERSIBLE OBSERVATORY
FOR BENTHIC STABILITY (SOBS)

FIGURE 3

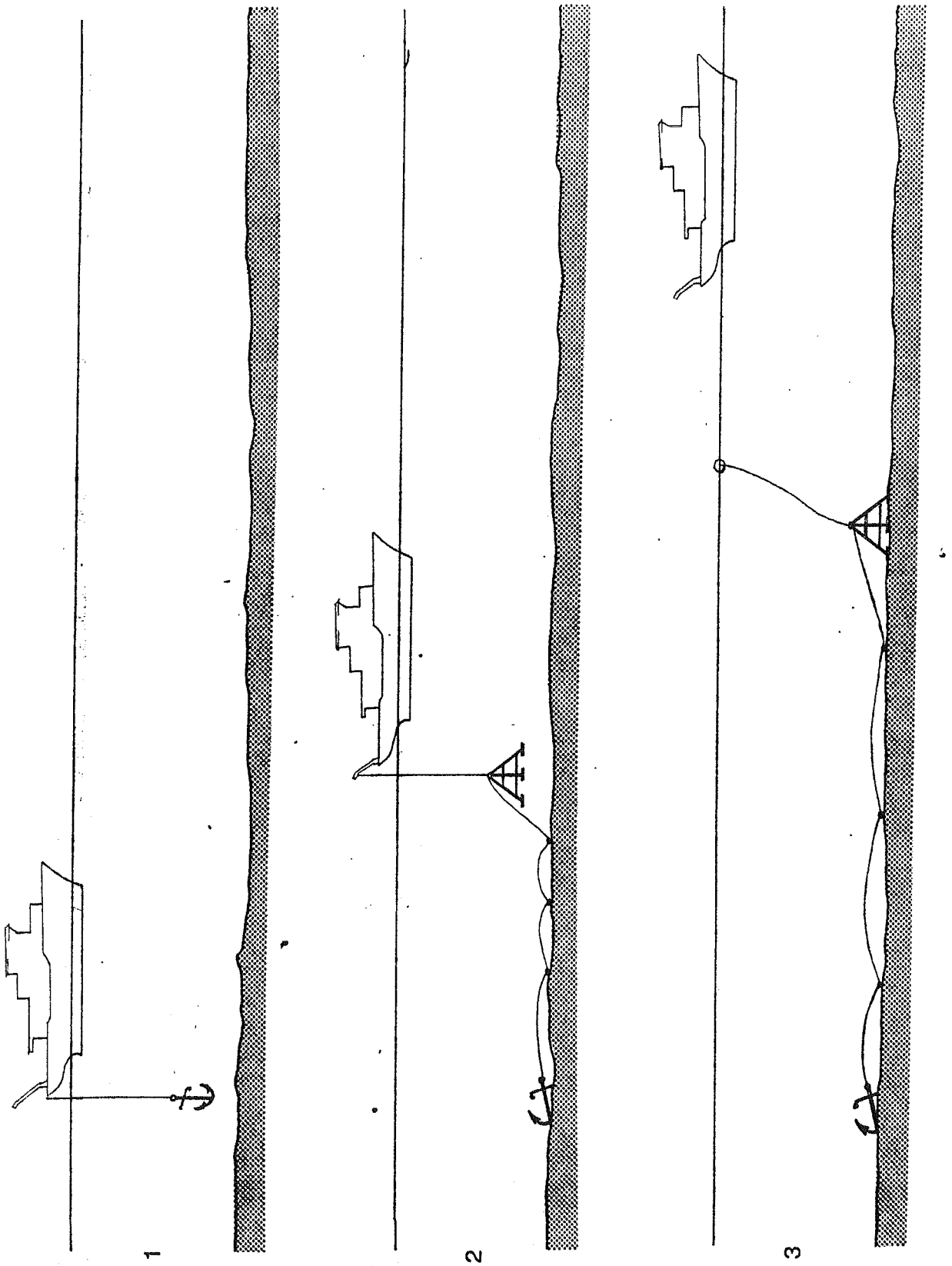

FIGURE 4

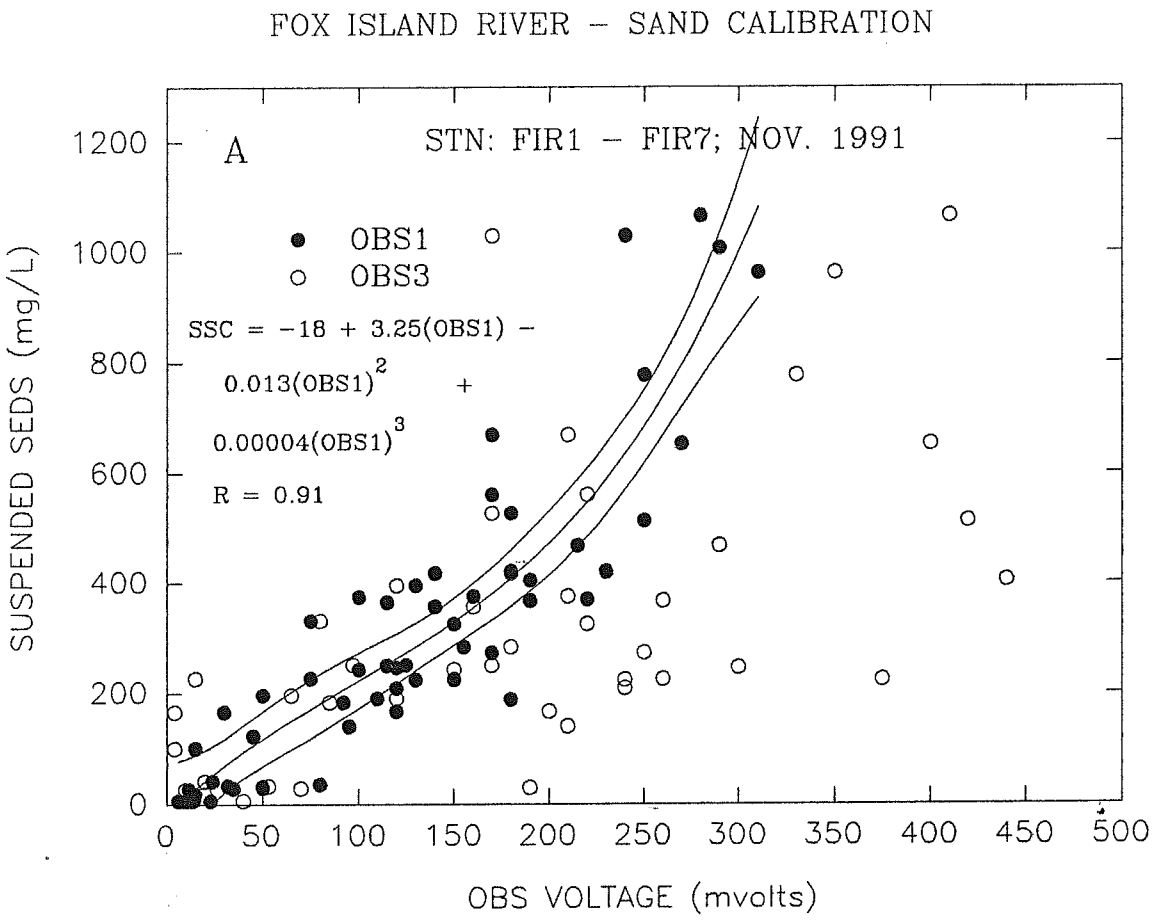
FOX ISLAND RIVER – SAND CALIBRATION
A
STN: FIR1 – FIR7; NOV. 1991
OBS1
OBS3
SSC = −18 + 3.25(OBS1) −
0.013(OBS1)^2 +
0.00004(OBS1)^3
R = 0.91
SUSPENDED SEDS (mg/L)
OBS VOLTAGE (mvolts)
0
200
400
600
800
1000
1200
0
50
100
150
200
250
300
350
400
450
500

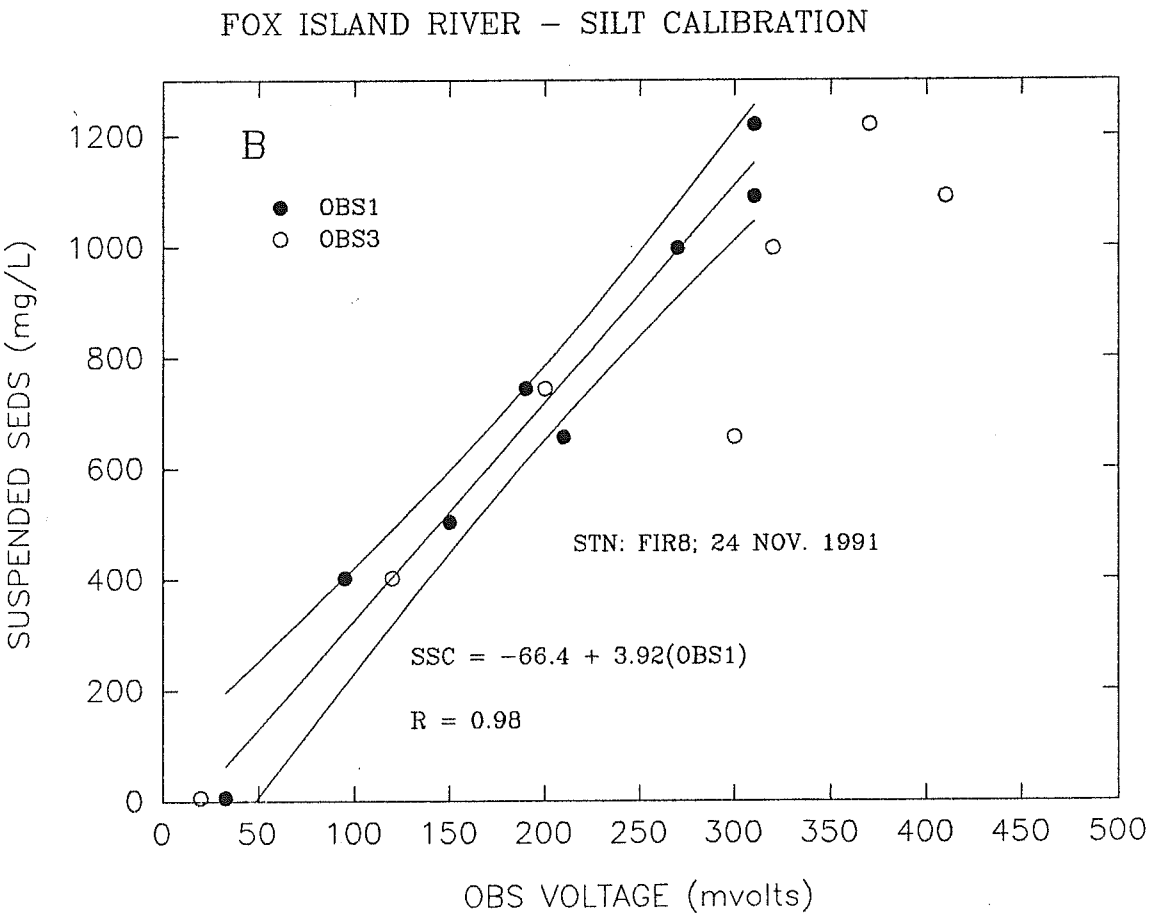
FOX ISLAND RIVER – SILT CALIBRATION
B
OBS1
OBS3
STN: FIR8; 24 NOV. 1991
SSC = −66.4 + 3.92(OBS1)
R = 0.98
SUSPENDED SEDS (mg/L)
OBS VOLTAGE (mvolts)
0
200
400
600
800
1000
1200
0
50
100
150
200
250
300
350
400
450
500

FIGURE 5

SEA CAROUSEL – FOX ISLAND RIVER, NFLD.

STATION FIR1 – 23 Nov. 1991

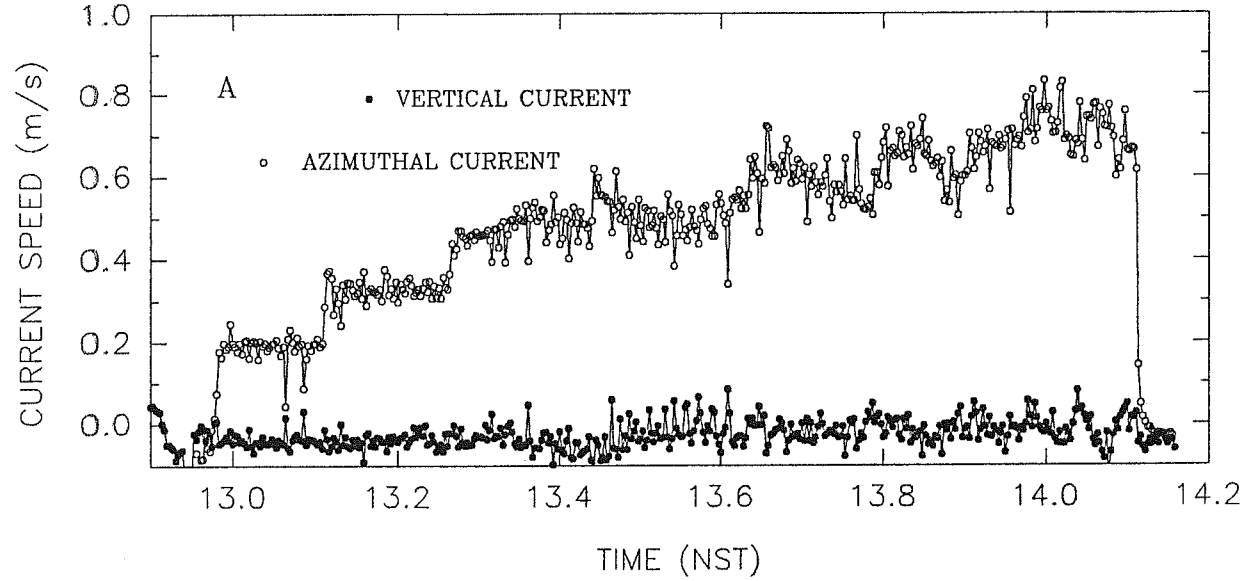

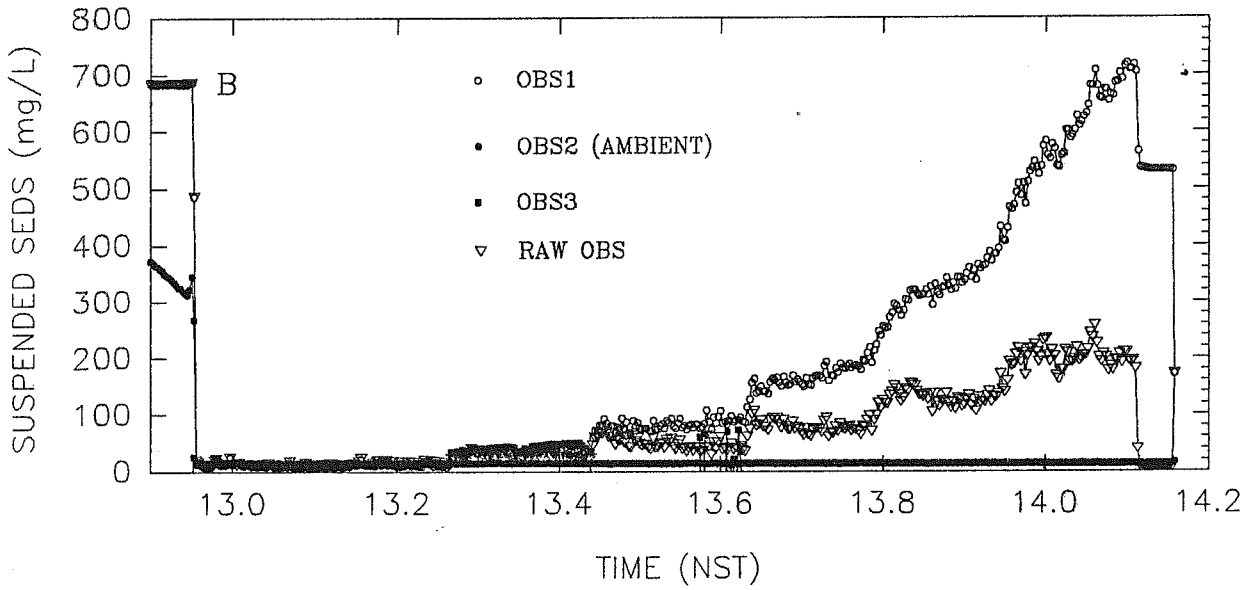

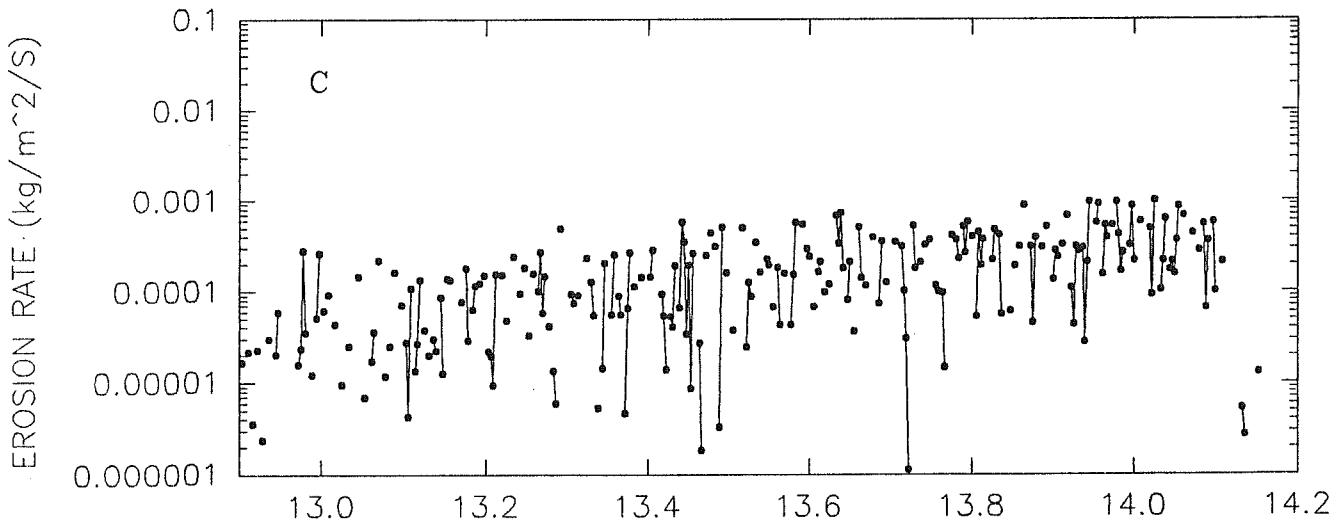

FIGURES 7 - 31

FOX ISLAND RIVER – NOV. 1991

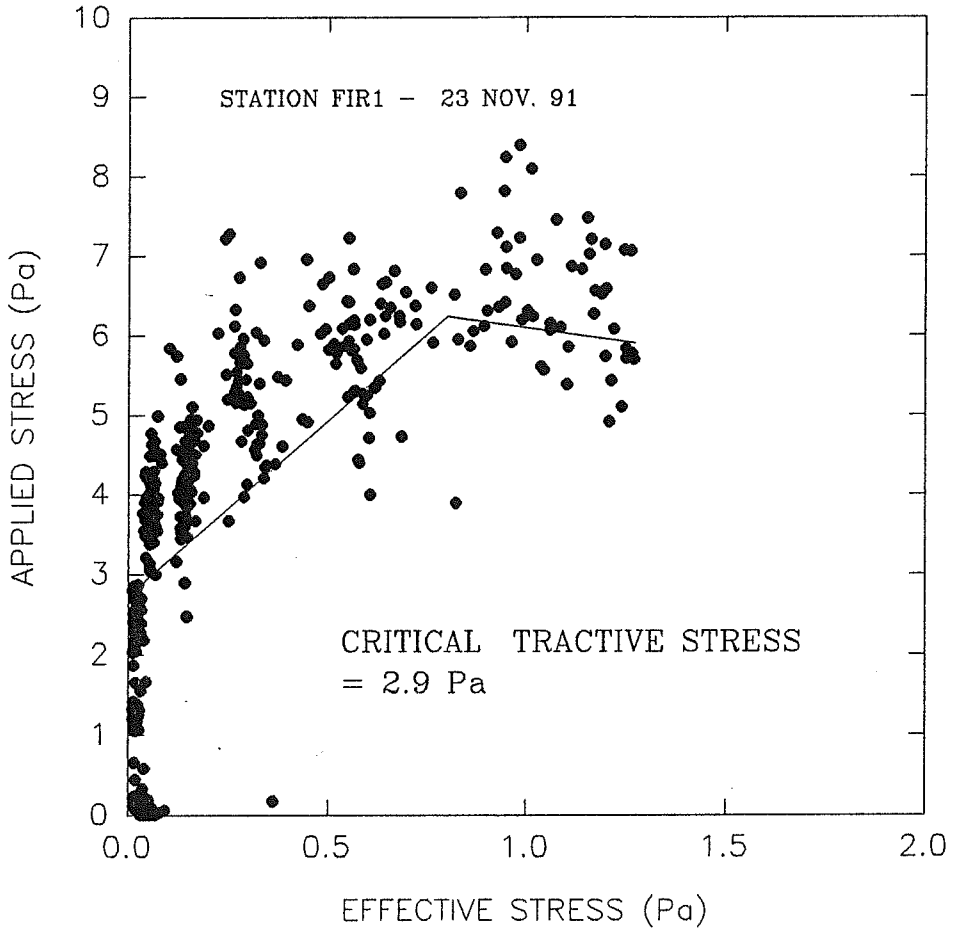

SEA CAROUSEL – FOX ISLAND RIVER, NFLD

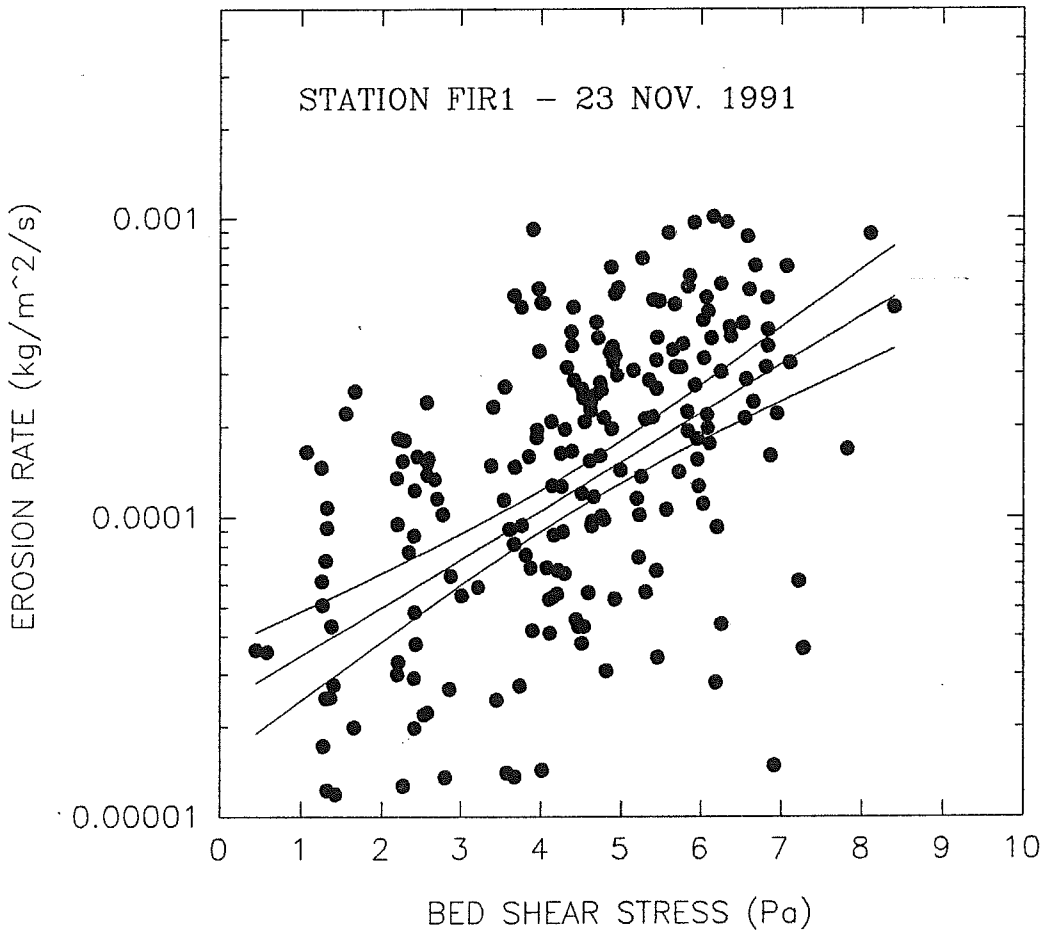

SEA CAROUSEL – FOX ISLAND RIVER, NFLD.

STATION FIR2 – 23 Nov. 1991

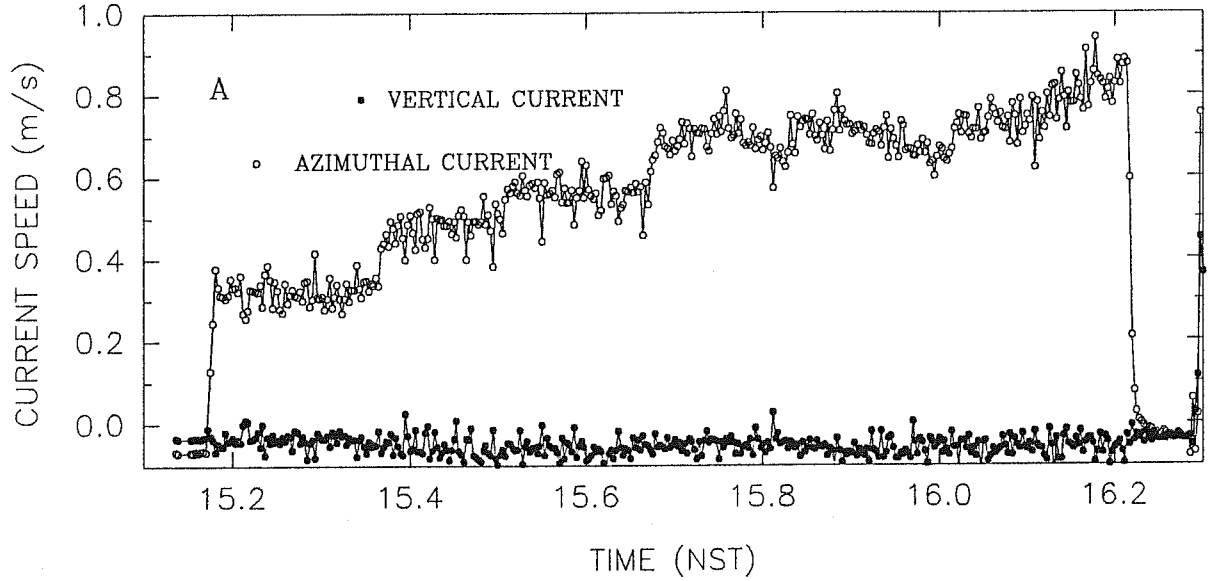

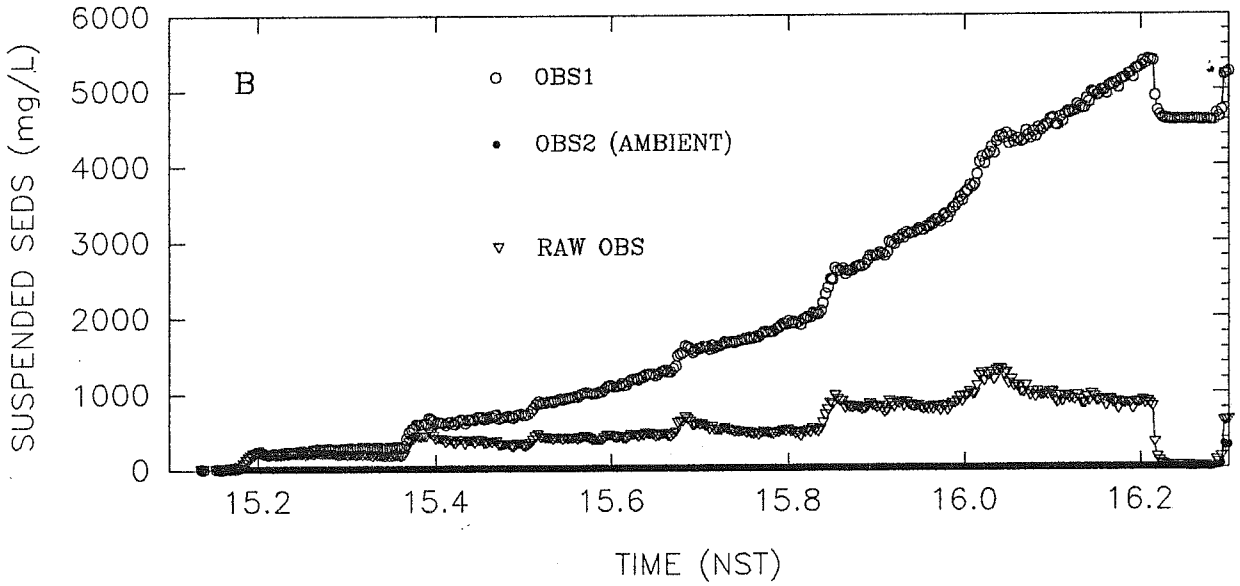

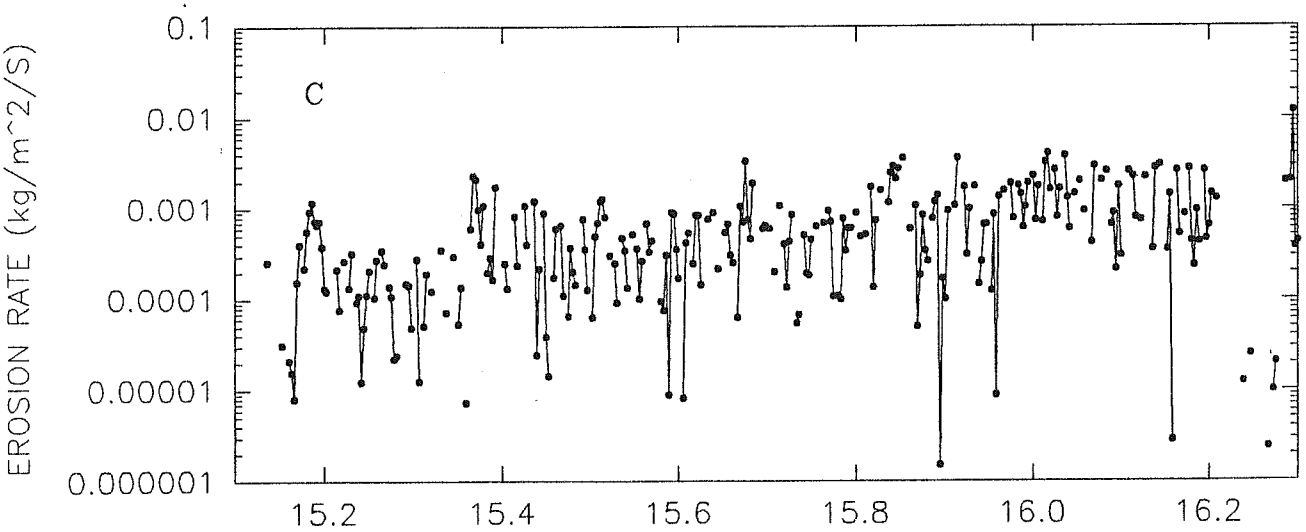

FOX ISLAND RIVER – NOV. 1991

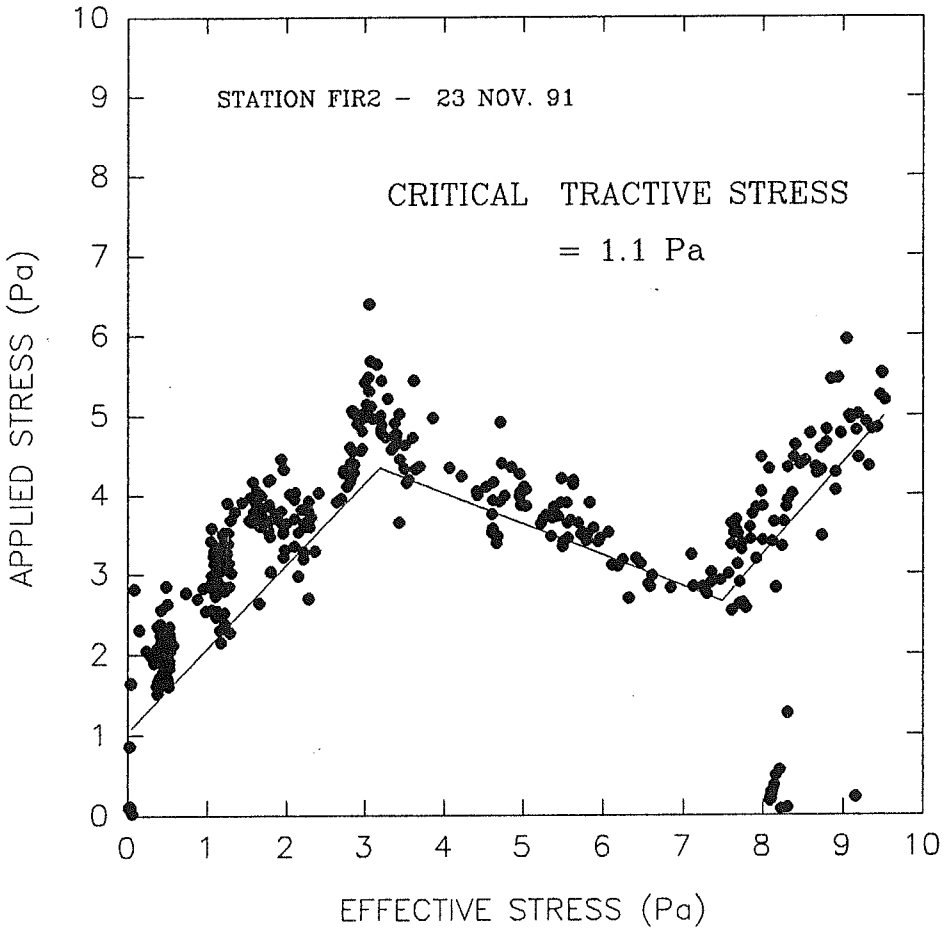

SEA CAROUSEL – FOX ISLAND RIVER – FIR2

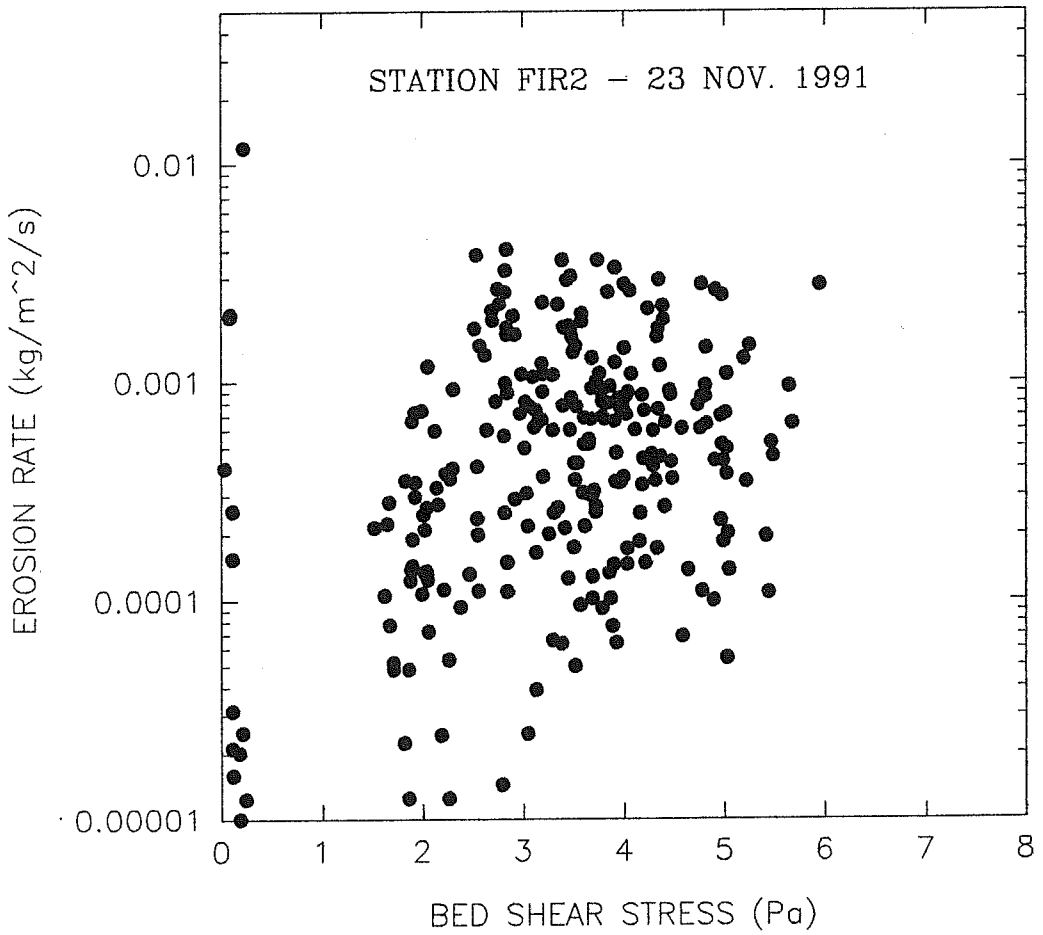

SEA CAROUSEL – FOX ISLAND RIVER, NFLD.

STATION FIR3 – 23 Nov. 1991

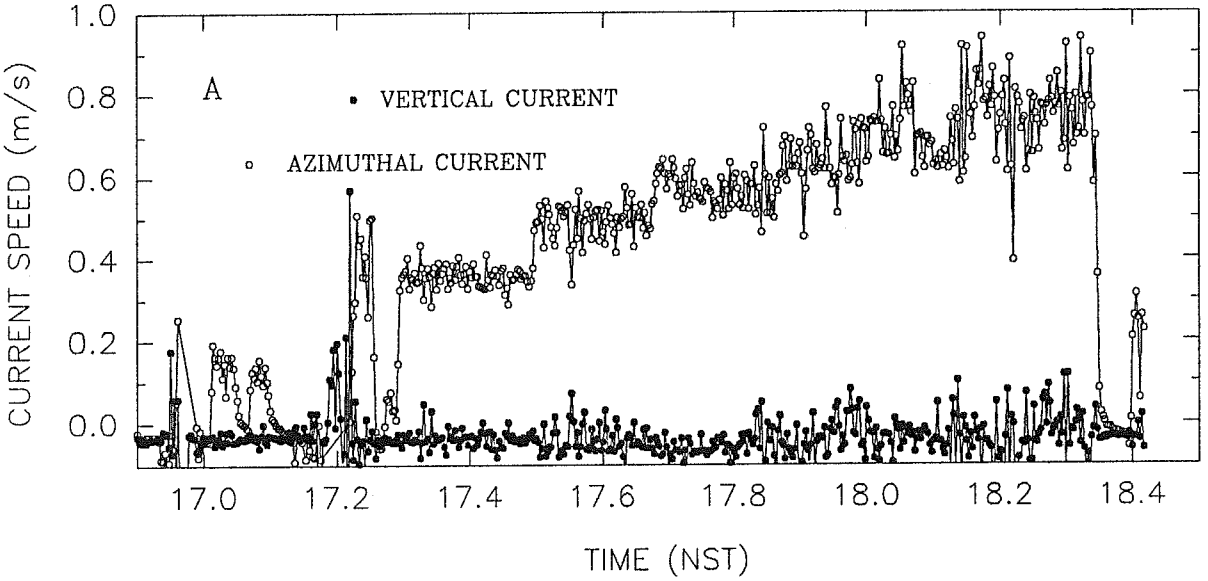

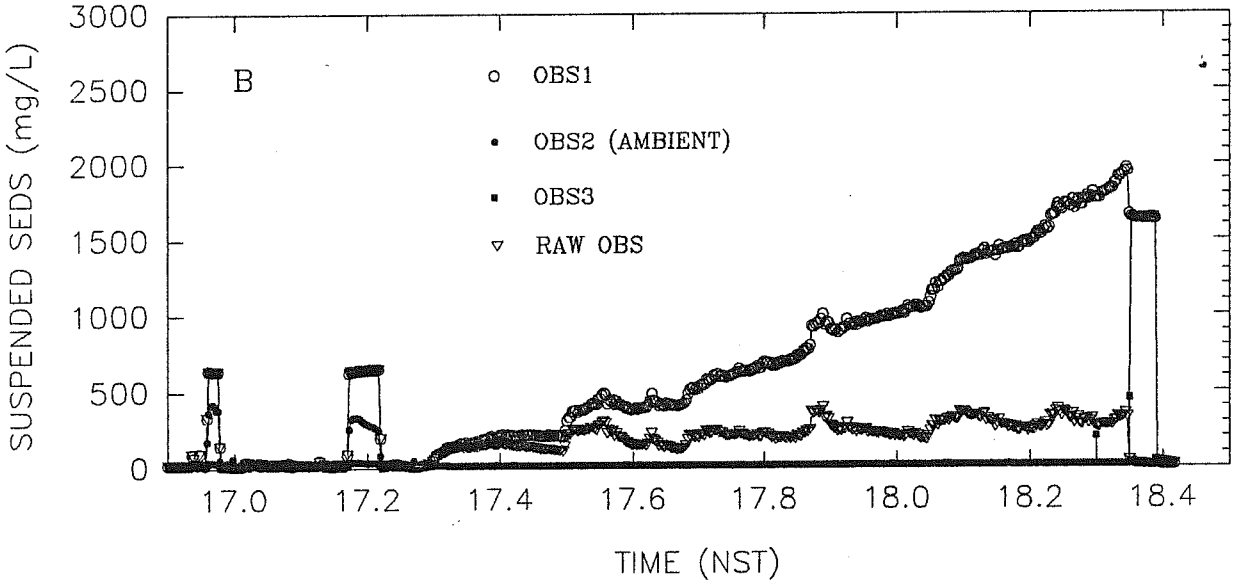

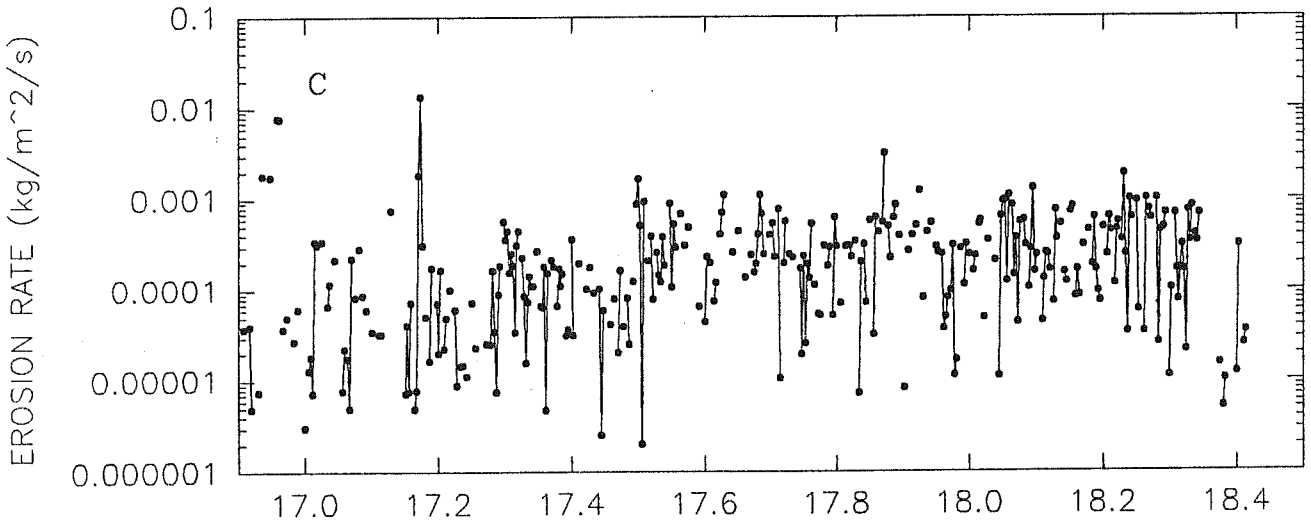

FOX ISLAND RIVER – NOV. 1991

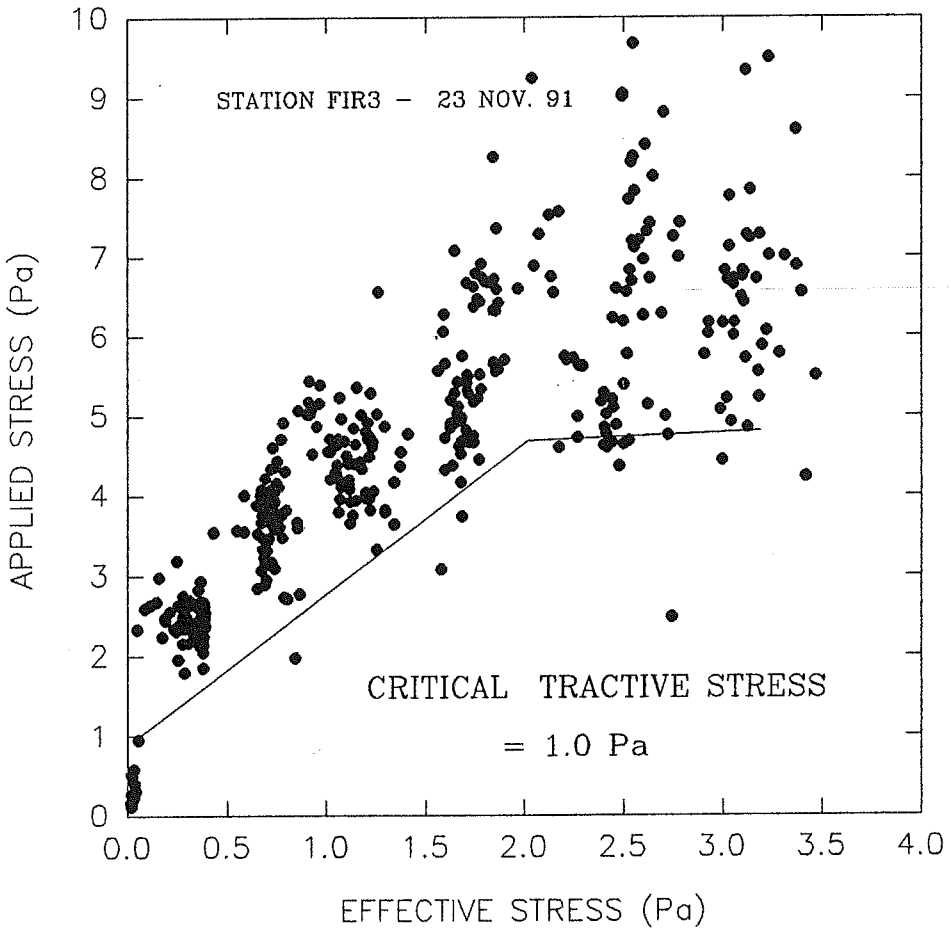

SEA CAROUSEL – FOX ISLAND RIVER – FIR3

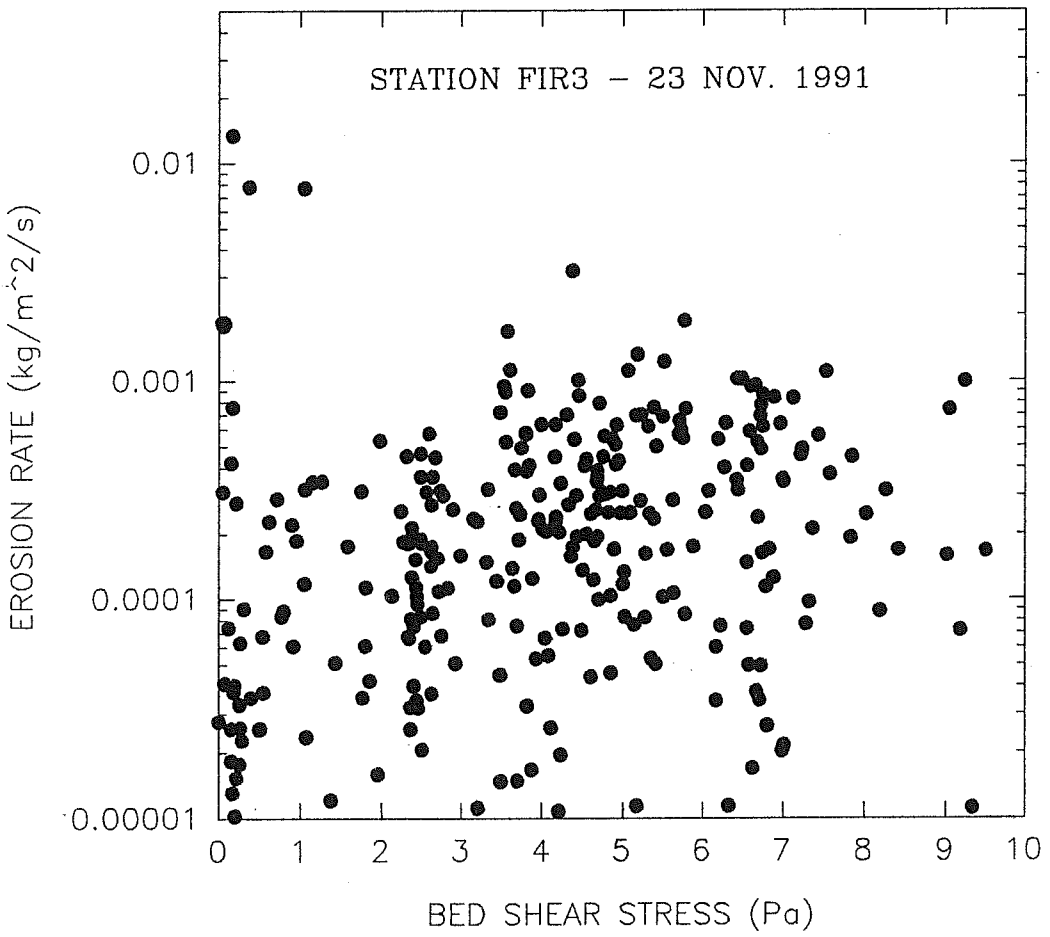

SEA CAROUSEL – FOX ISLAND RIVER, NFLD.

STATION FIR4 – 23 Nov. 1991

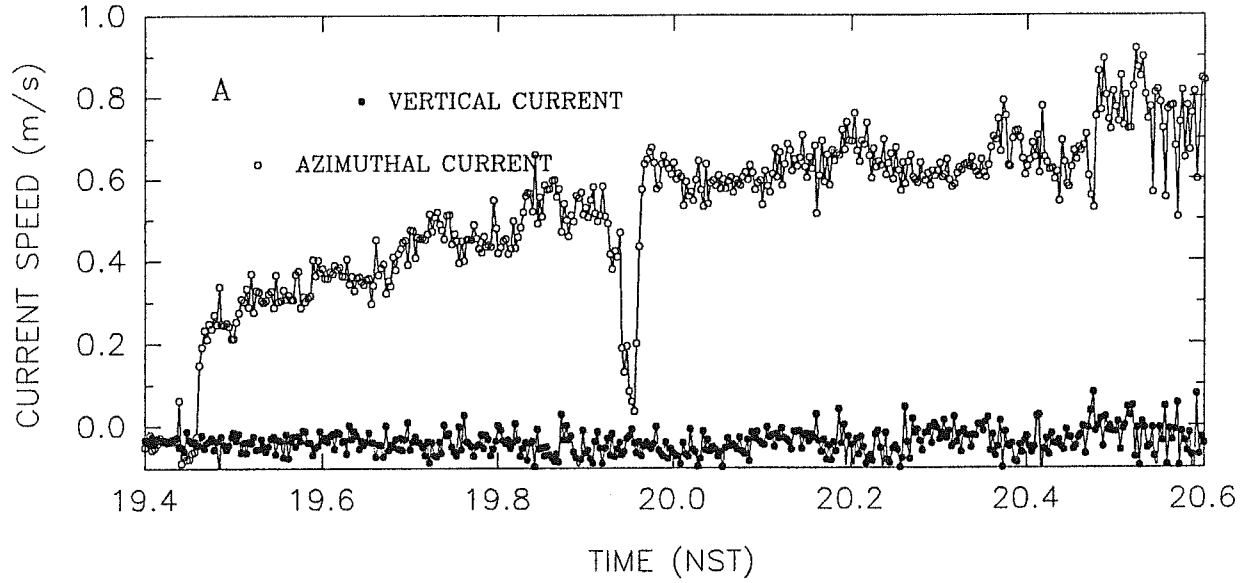

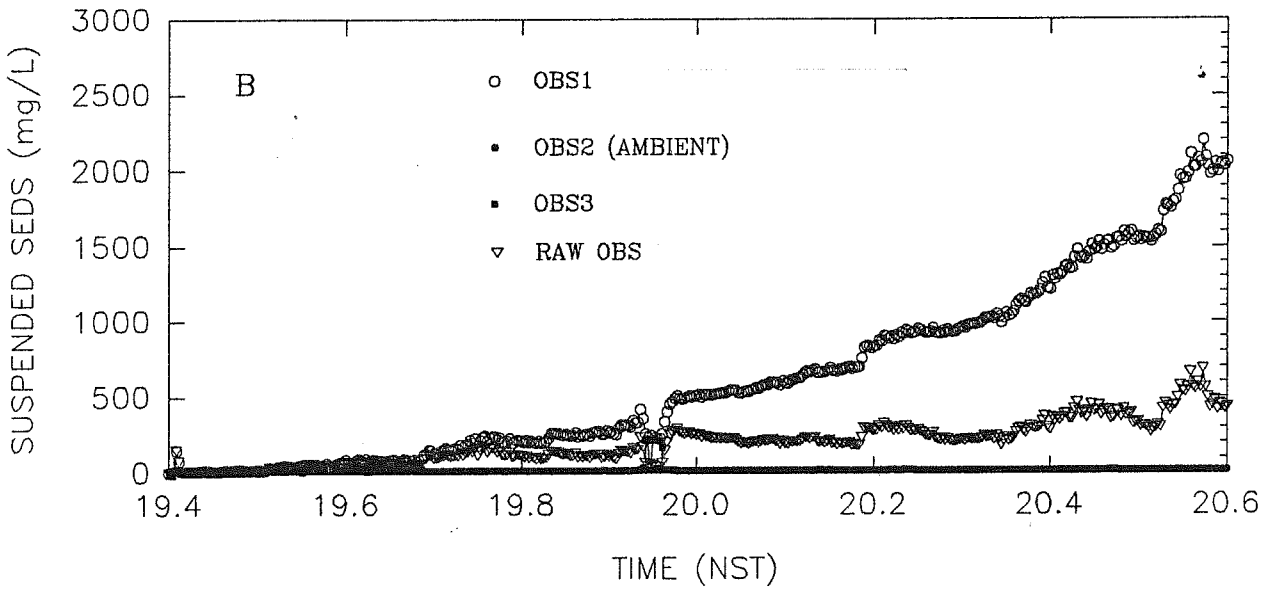

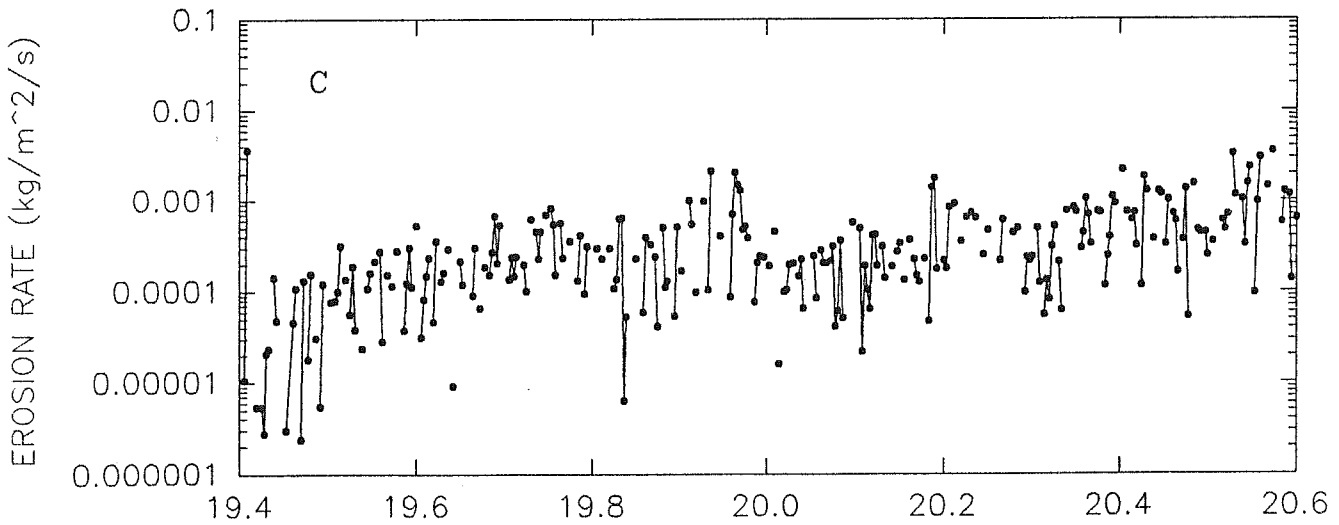

FOX ISLAND RIVER – NOV. 1991

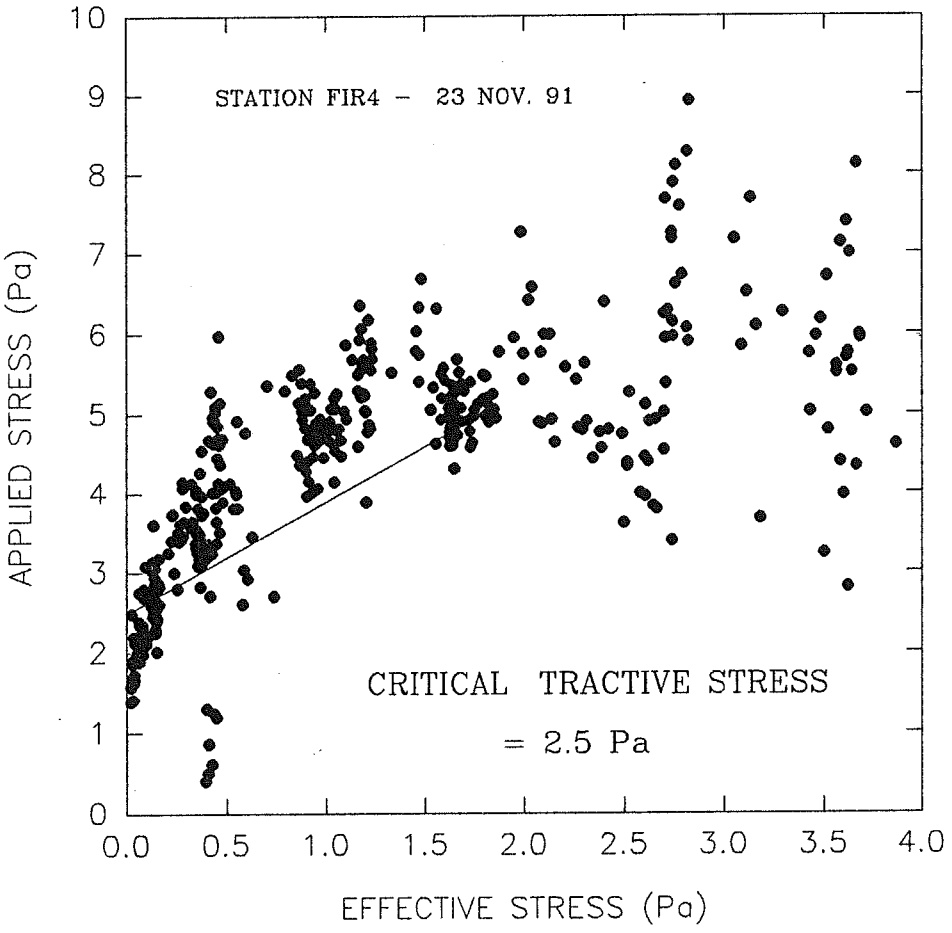

SEA CAROUSEL – FOX ISLAND RIVER – FIR4

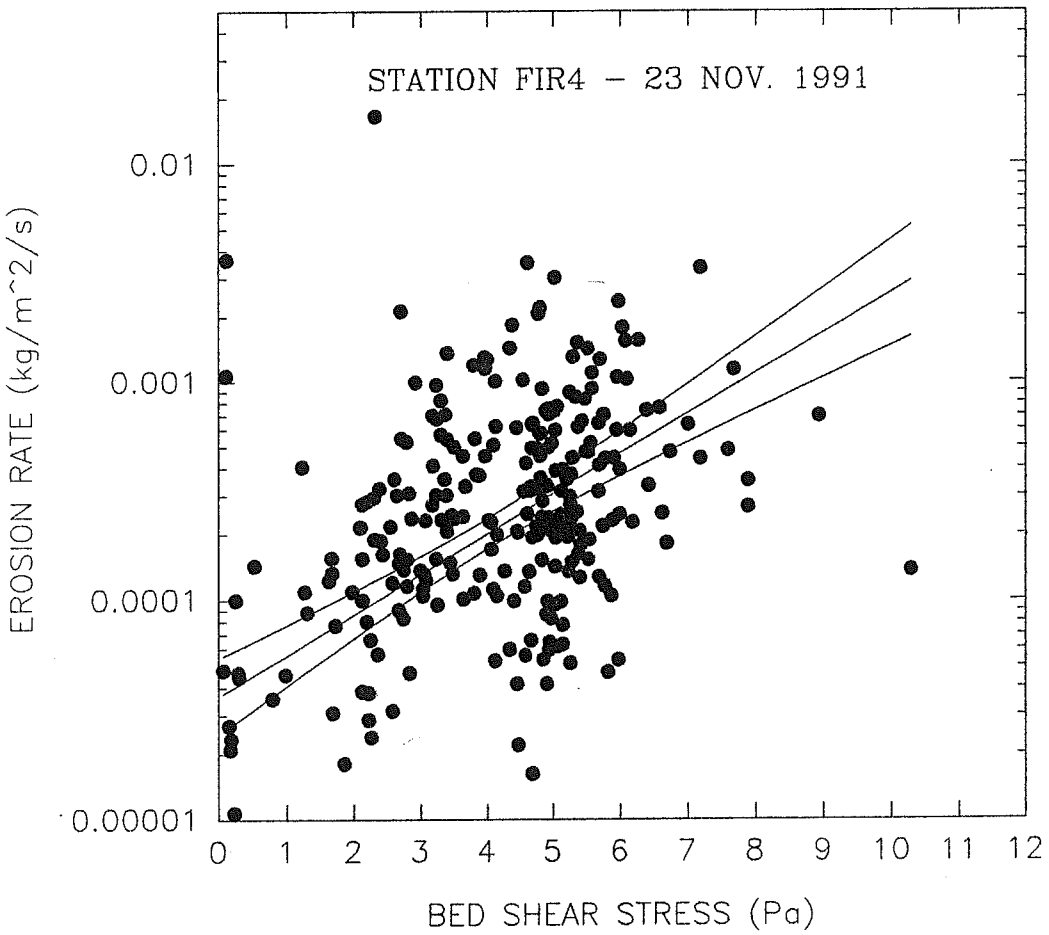

SEA CAROUSEL – FOX ISLAND RIVER, NFLD.

STATION FIR5 – 24 Nov. 1991

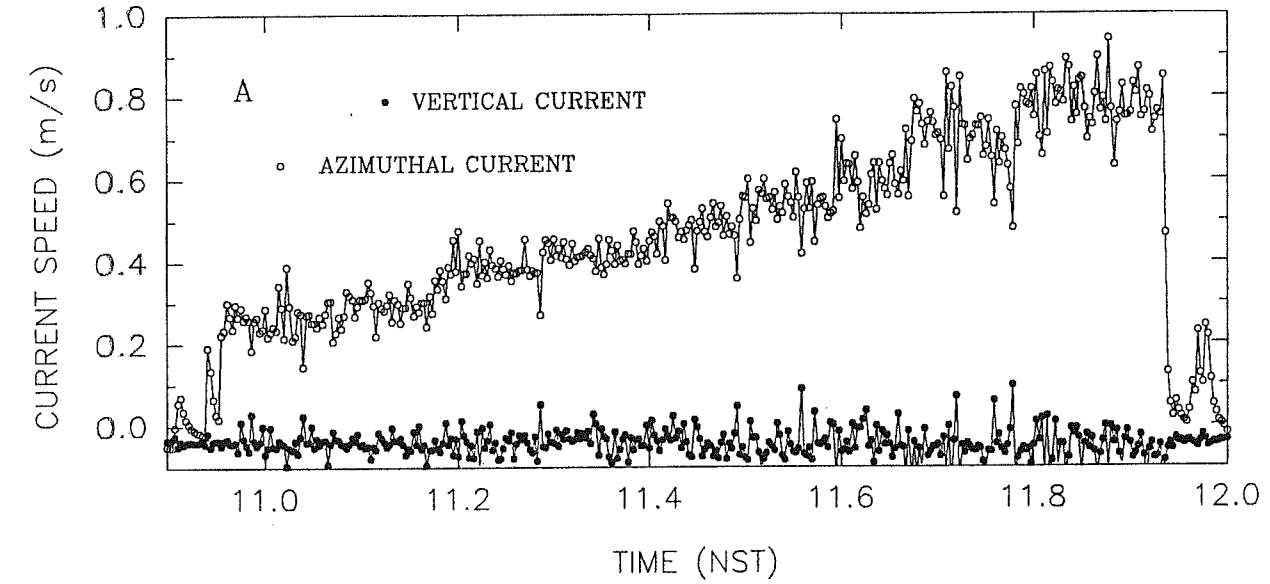

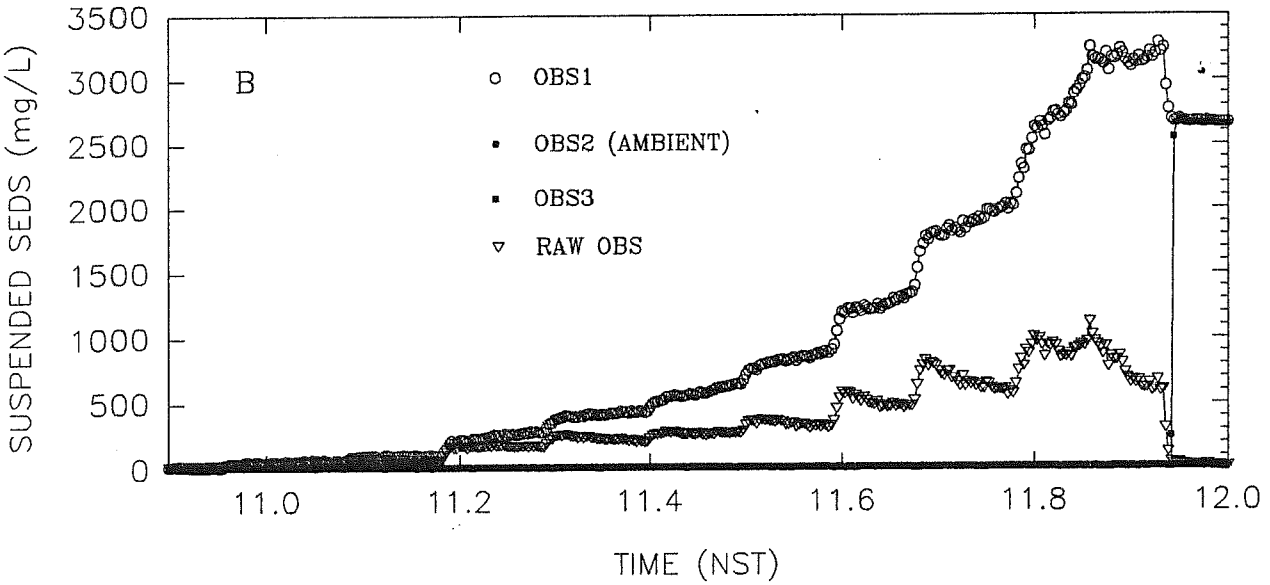

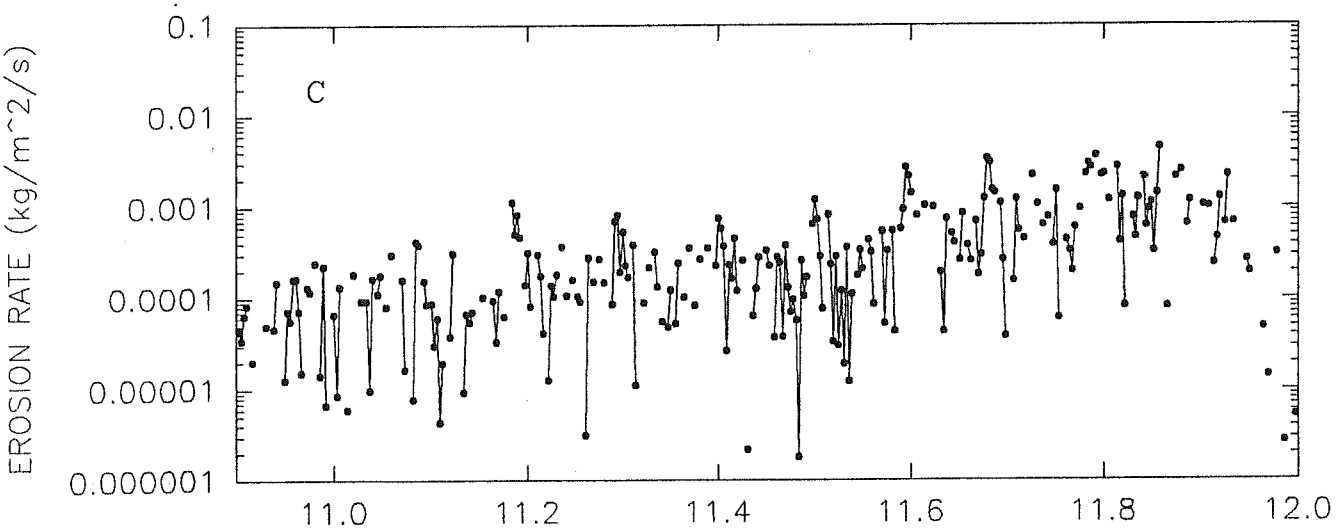

FOX ISLAND RIVER – NOV. 1991

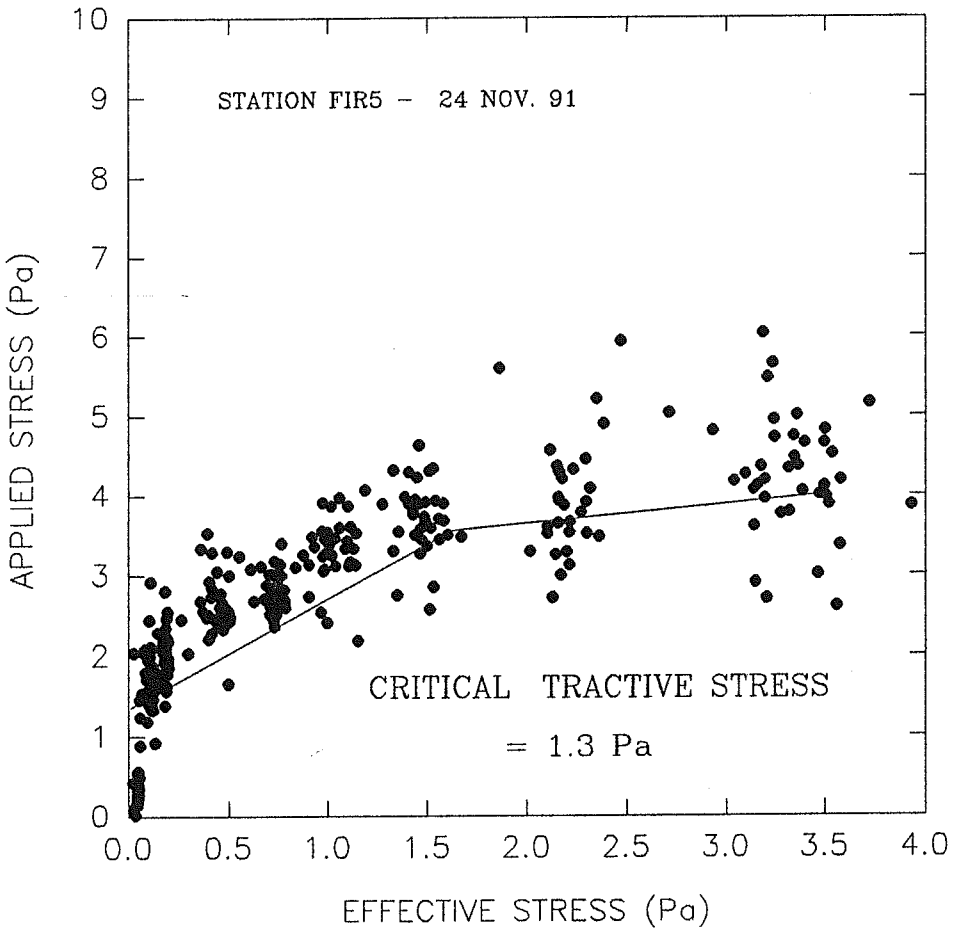

SEA CAROUSEL – FOX ISLAND RIVER – FIR5

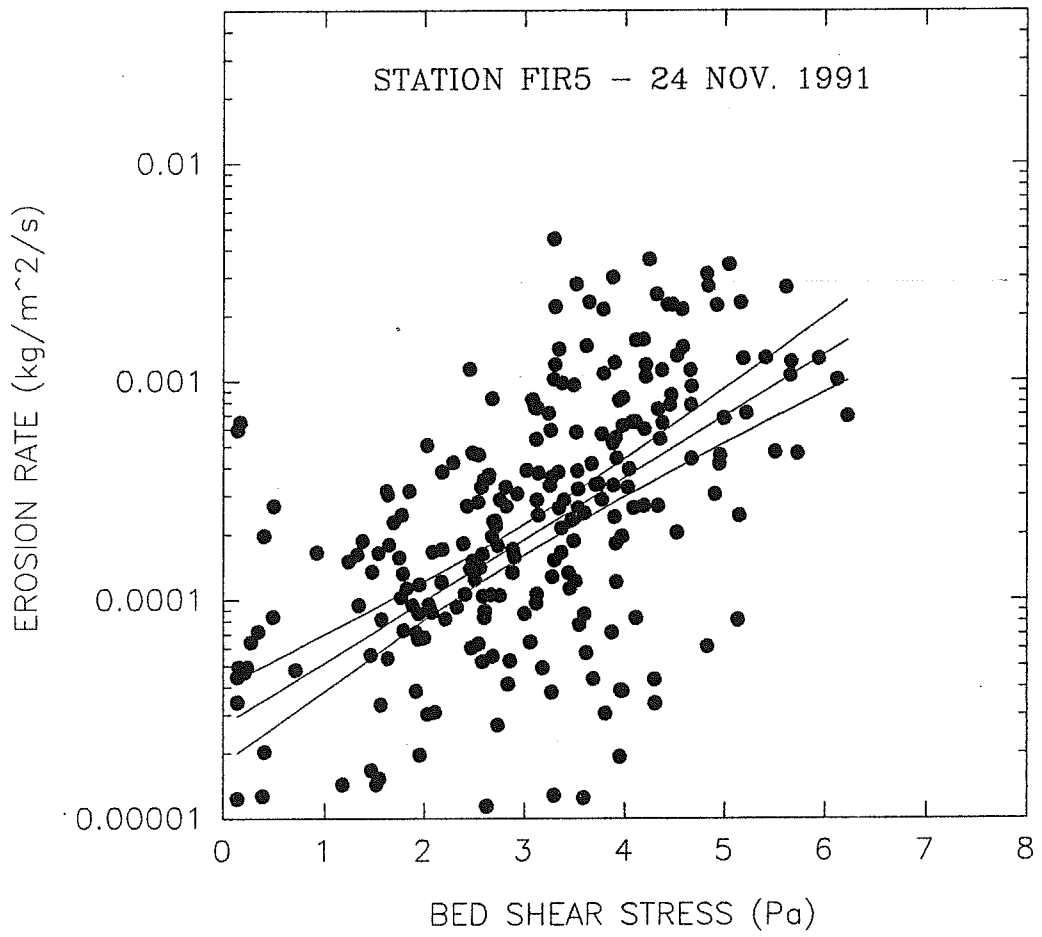

SEA CAROUSEL – FOX ISLAND RIVER, NFLD.

STATION FIR6 – 24 Nov. 1991

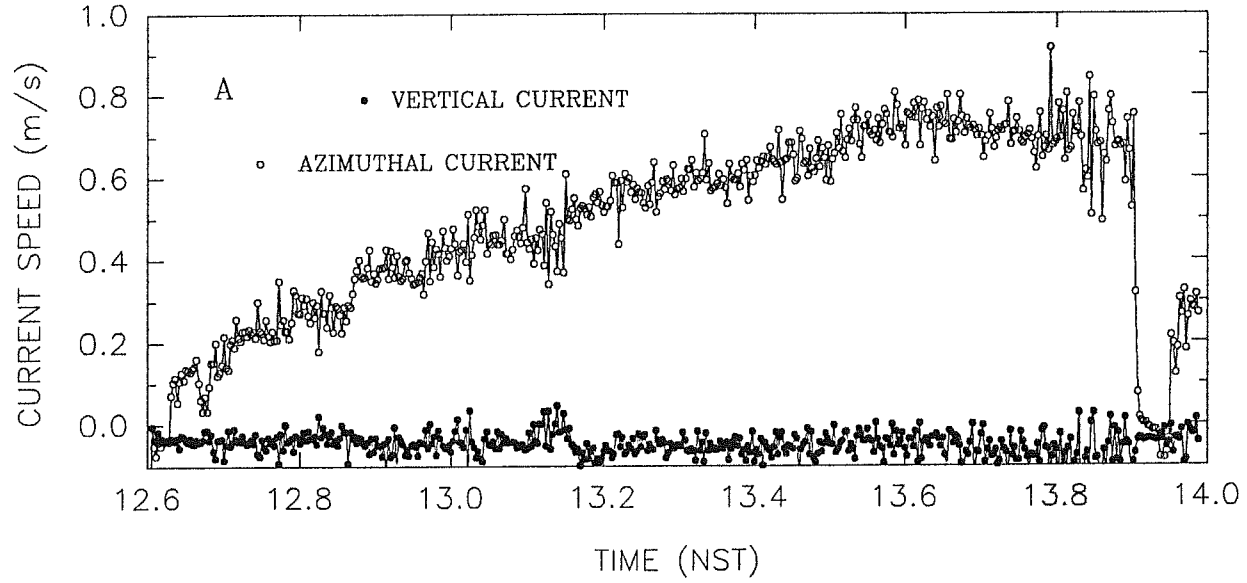

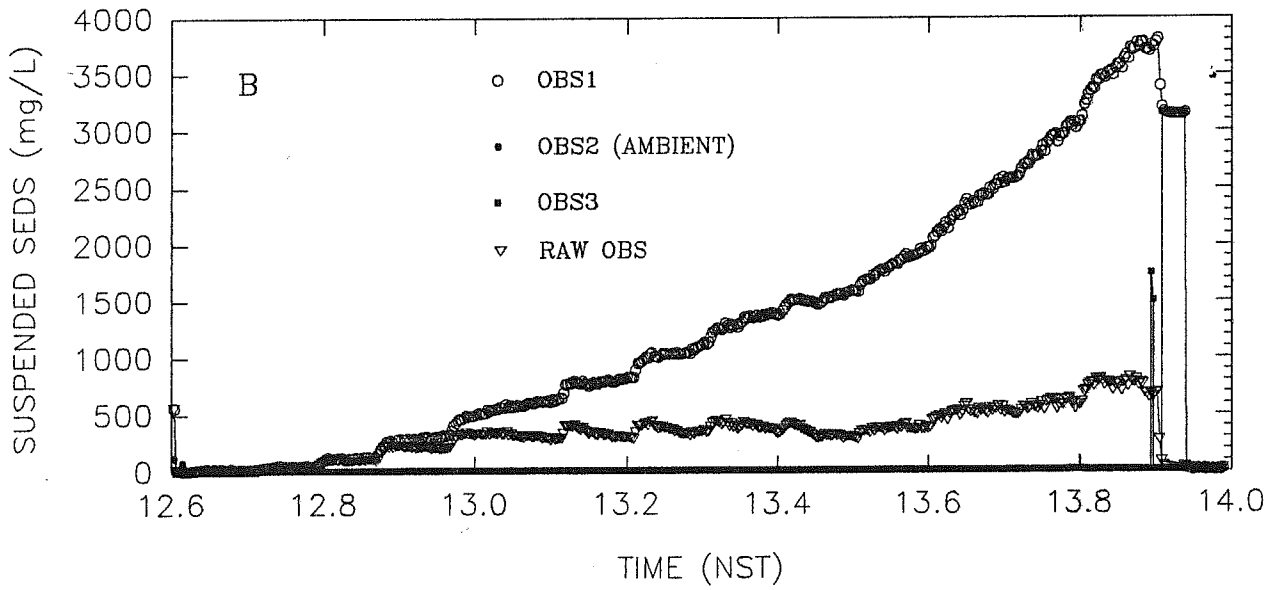

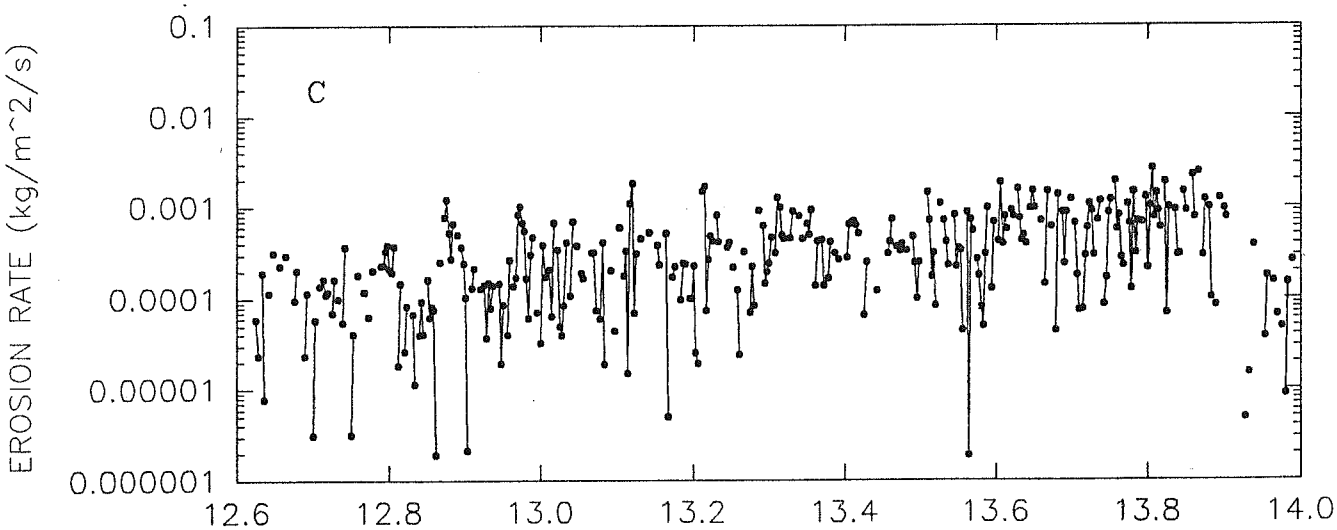

FOX ISLAND RIVER – NOV. 1991

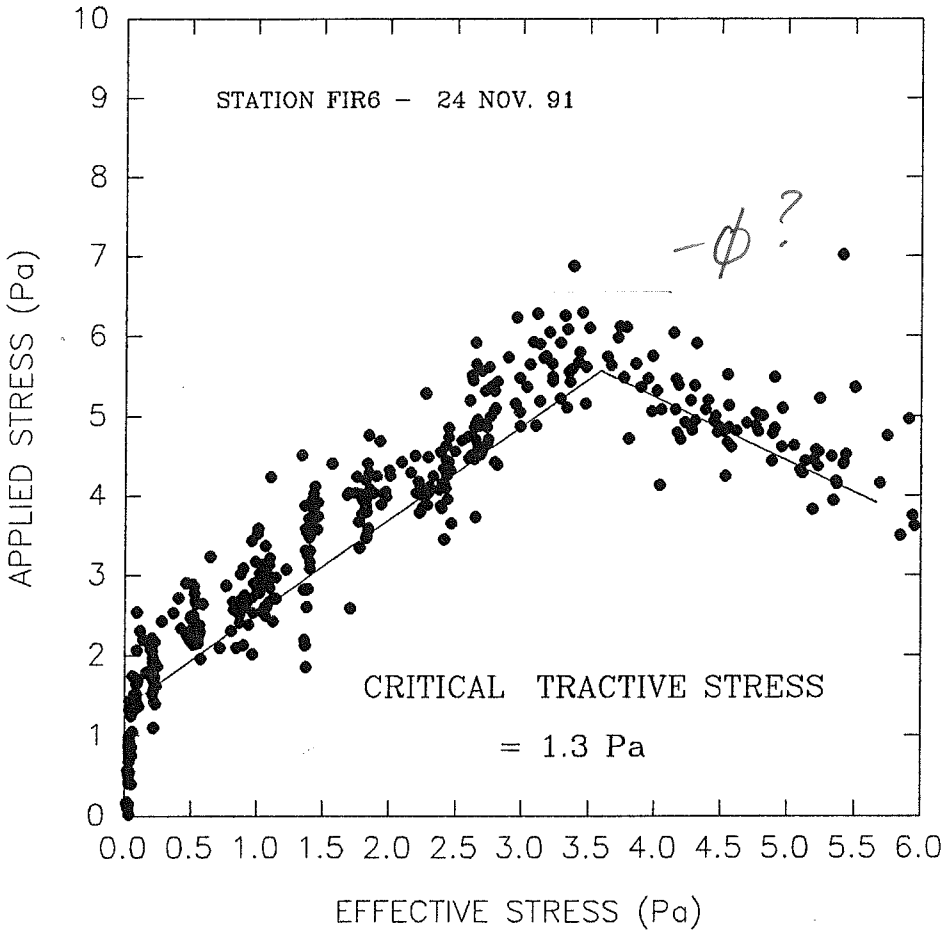

SEA CAROUSEL – FOX ISLAND RIVER – FIR6

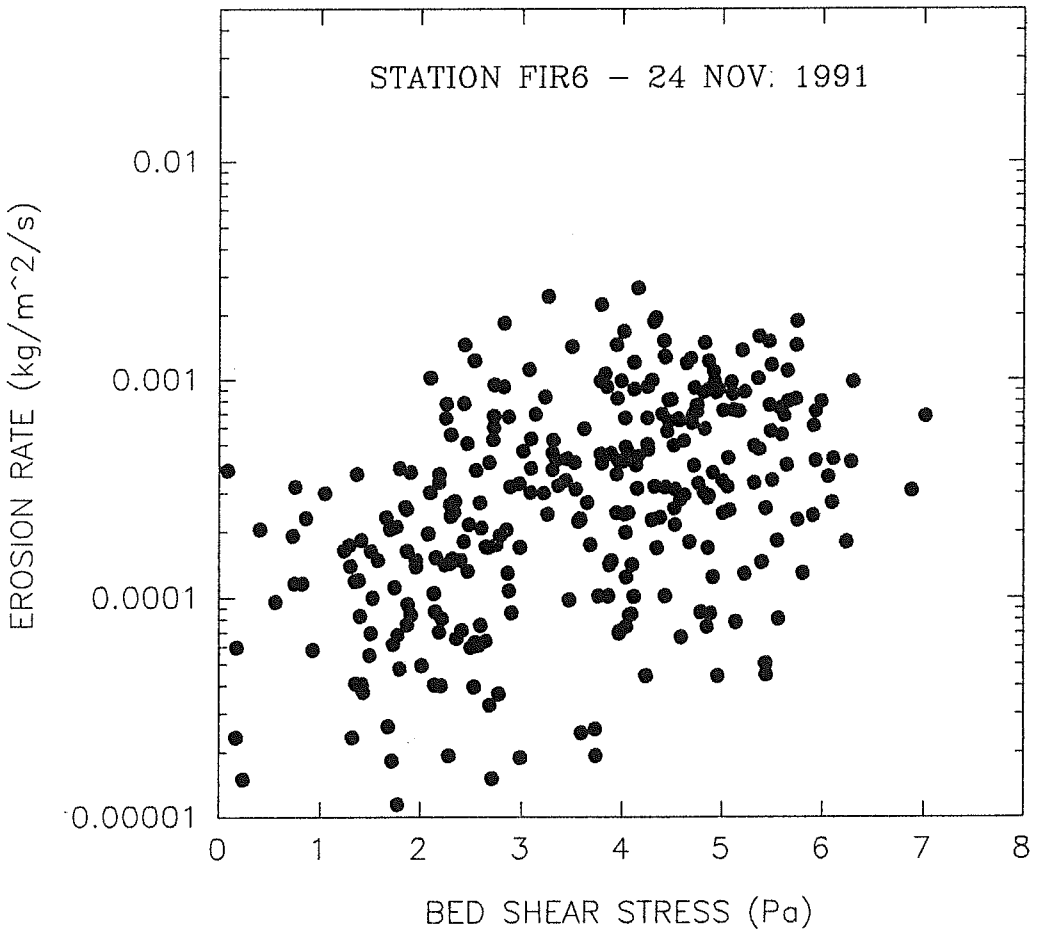

SEA CAROUSEL – FOX ISLAND RIVER, NFLD.

STATION FIR7 – 24 Nov. 1991

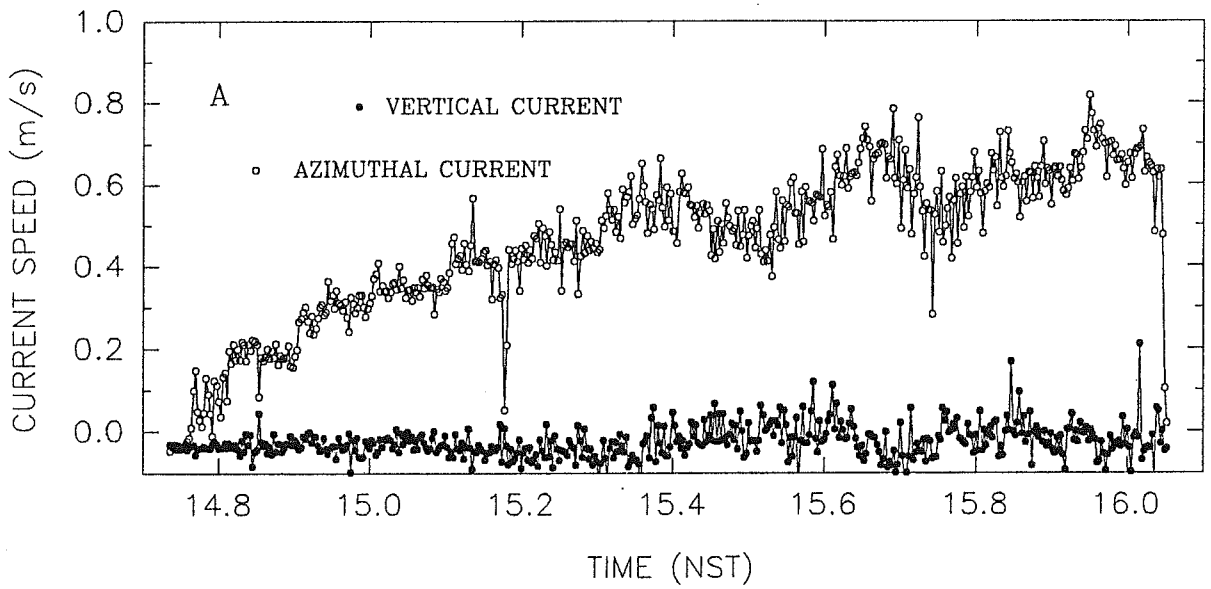

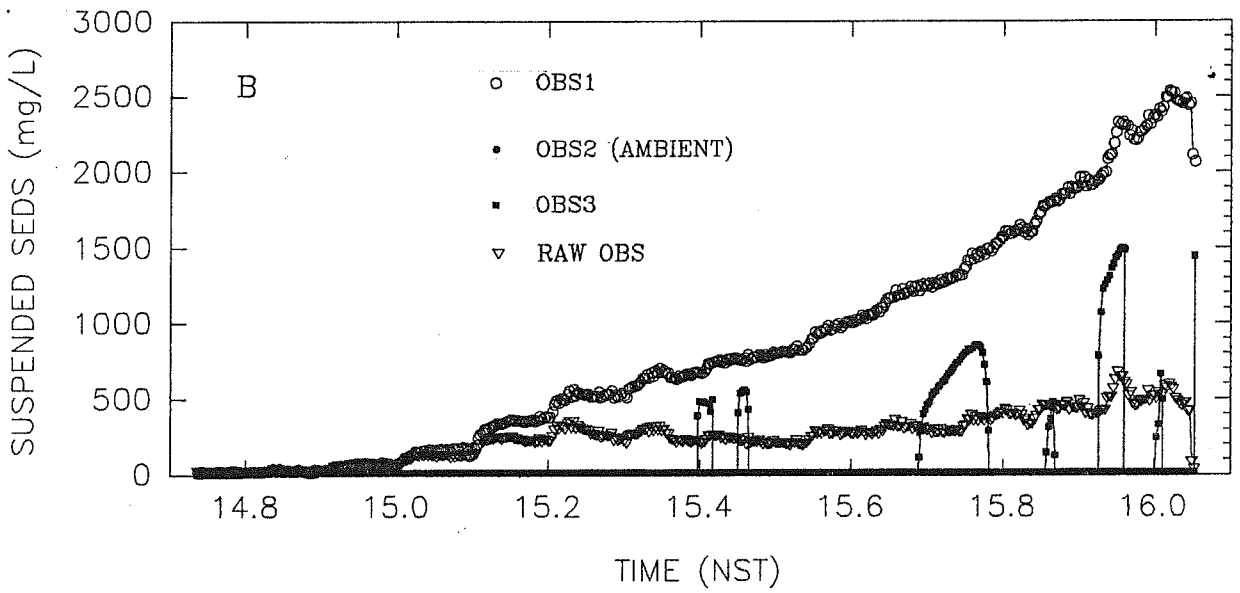

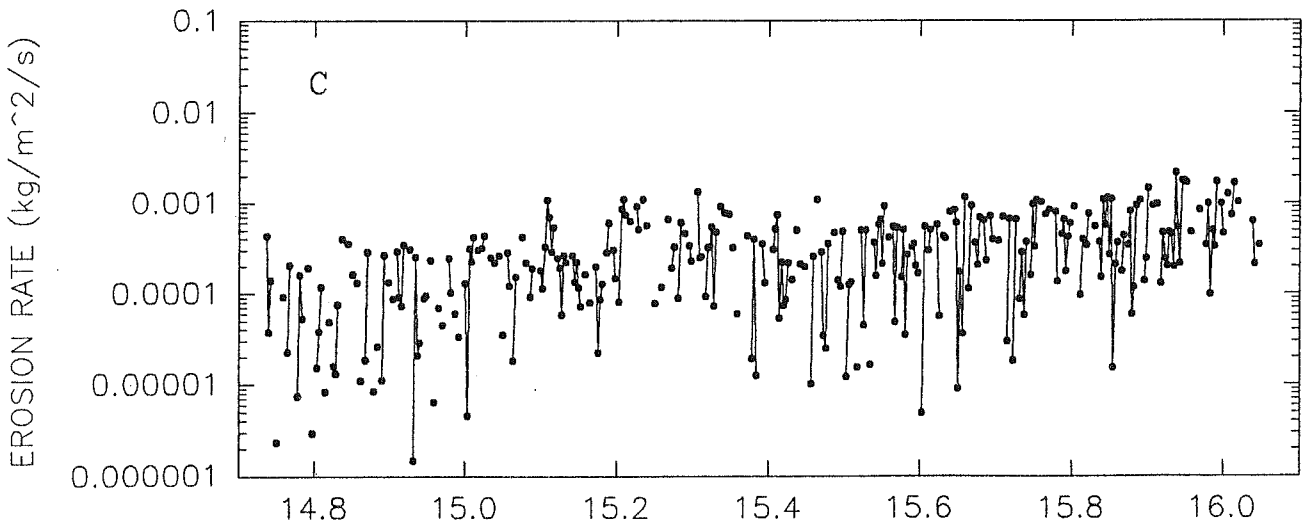

FOX ISLAND RIVER – NOV. 1991

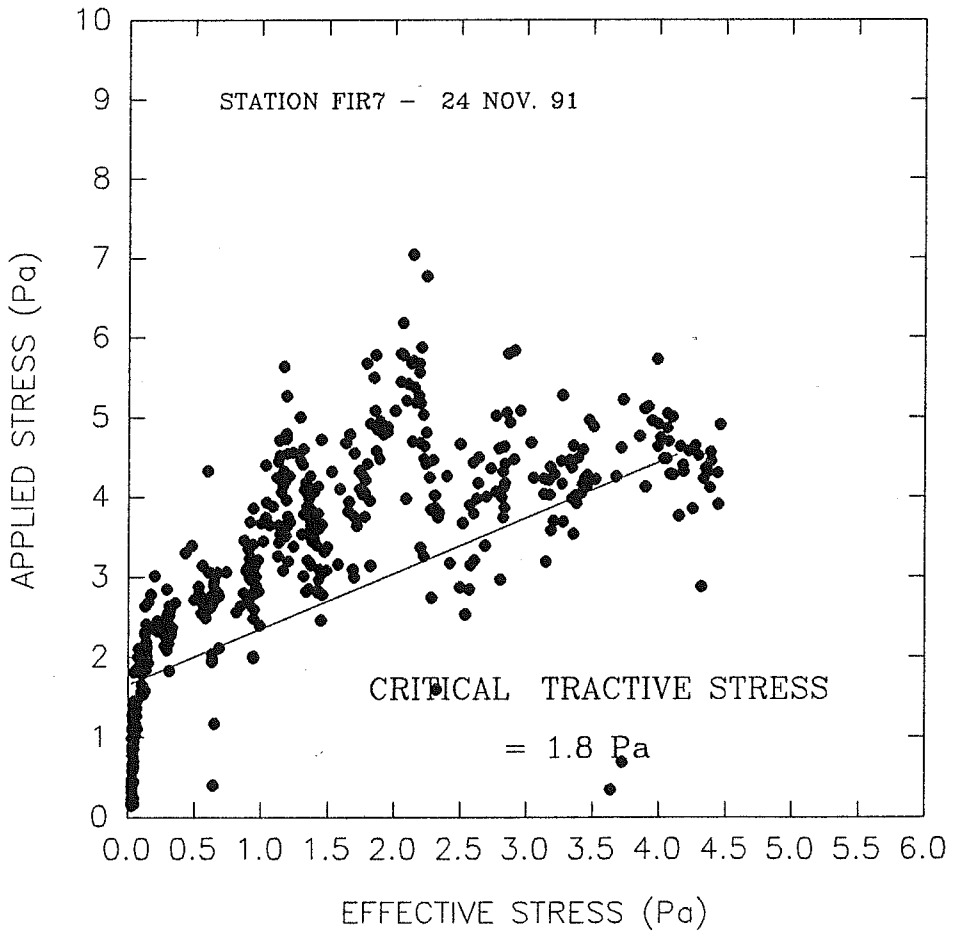

SEA CAROUSEL – FOX ISLAND RIVER – FIR7

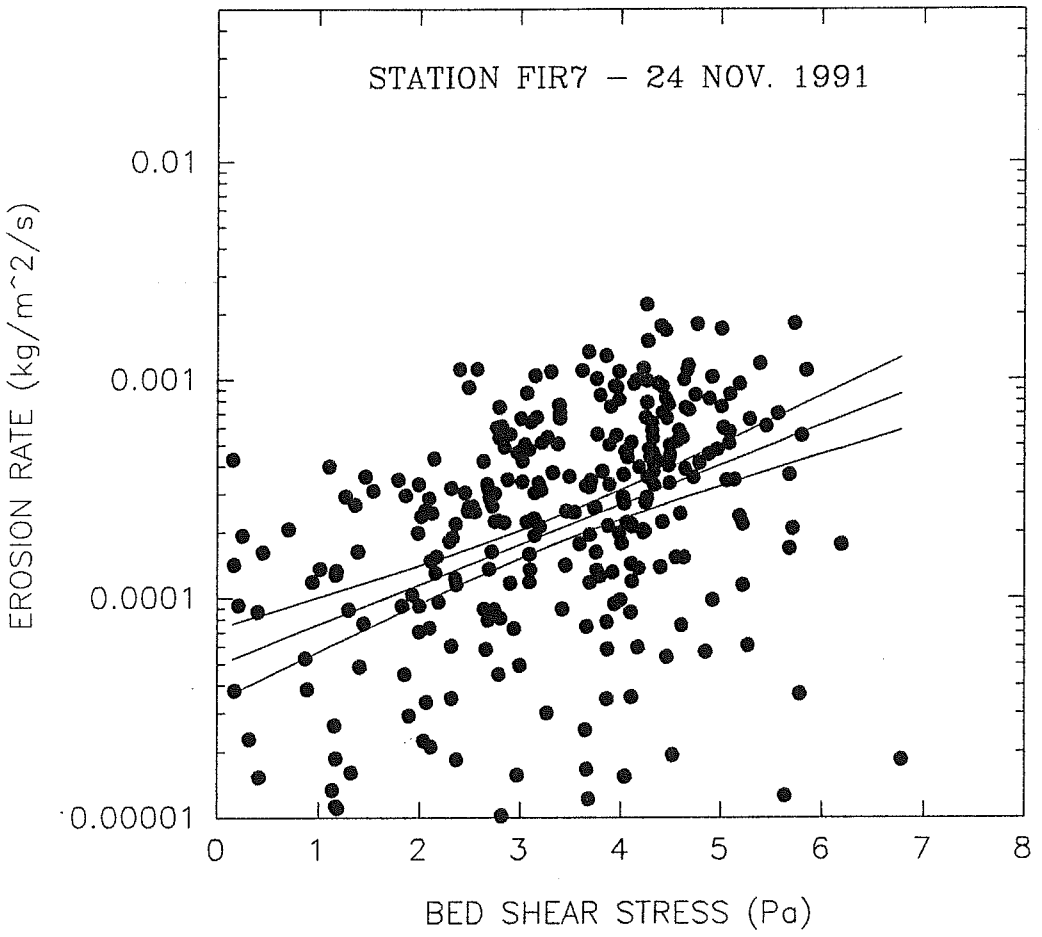

SEA CAROUSEL – FOX ISLAND RIVER, NFLD.

STATION FIR8 – 24 Nov. 1991

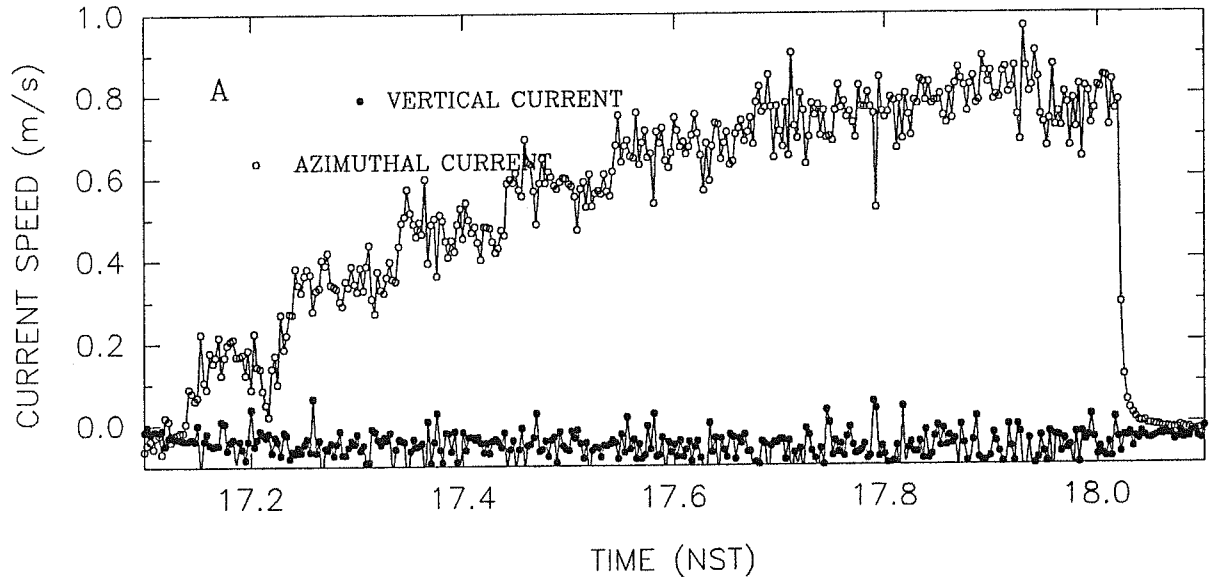

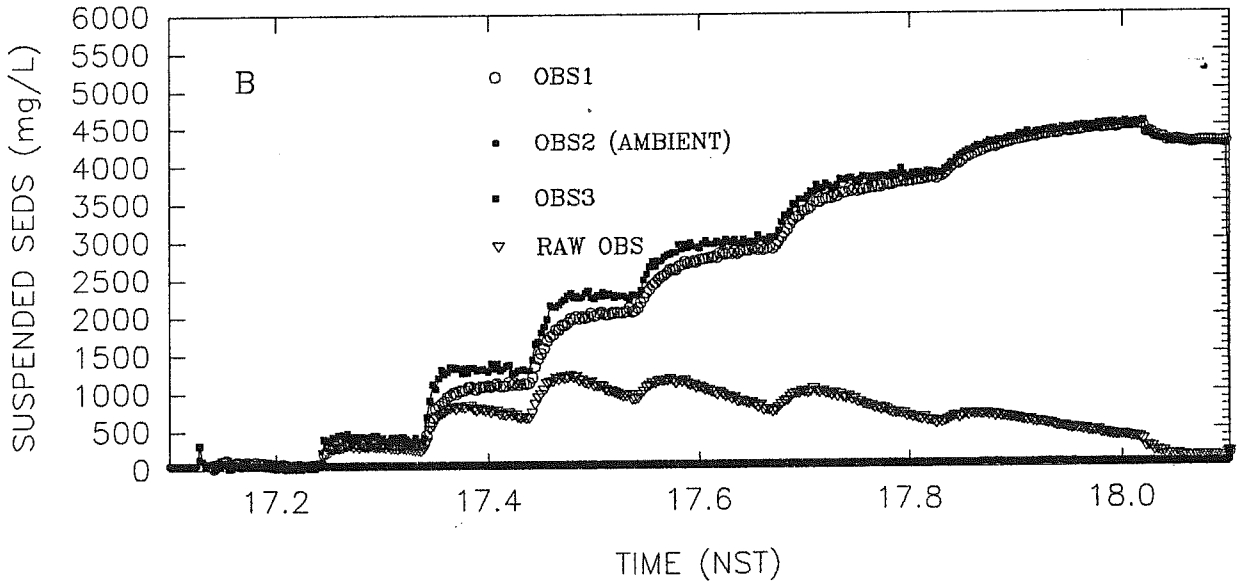

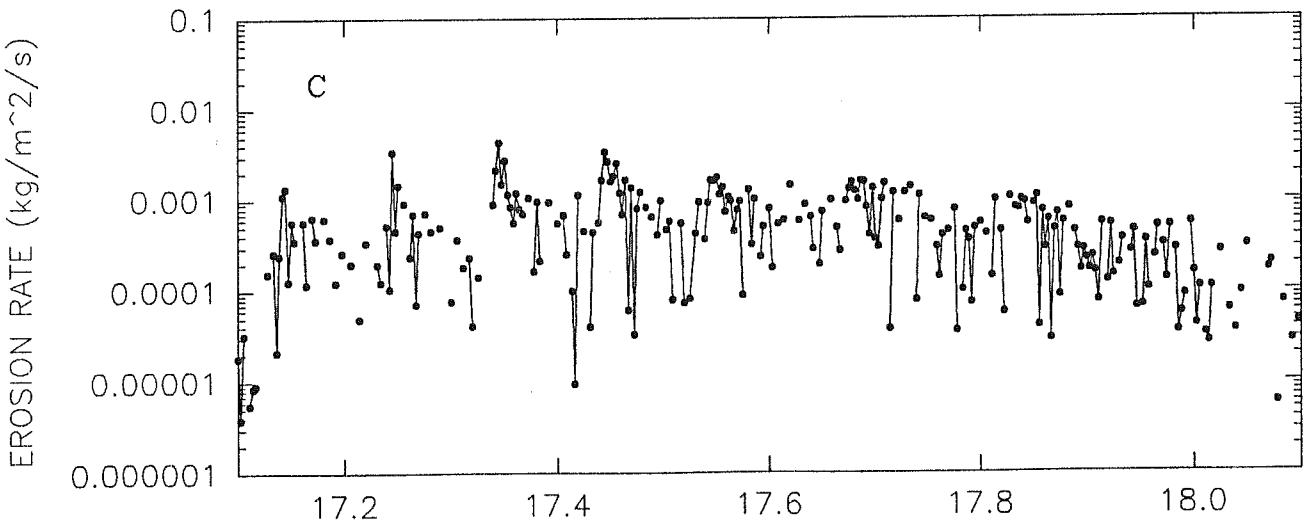

FOX ISLAND RIVER – NOV. 1991

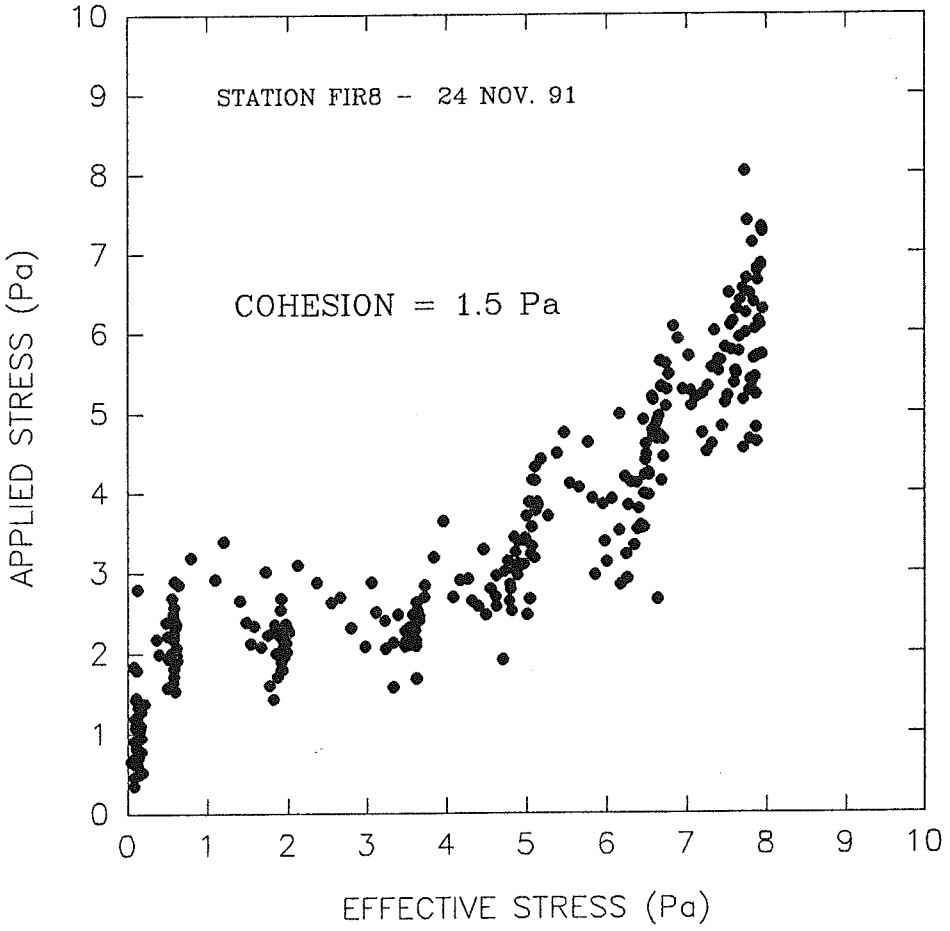

SEA CAROUSEL – FOX ISLAND RIVER – FIR8